THE HARMONIC EXCITATION OF A CYLINDRICAL BUBBLE PINNED TO A PLANE SURFACE: FLOW FIELD AND OSCILLATION DYNAMICS

BY

VENKATARAMA BHARGAV RALLABANDI

THESIS

Submitted in partial fulfillment of the requirements
for the degree of Master of Science in Theoretical and Applied Mechanics
in the Graduate College of the
University of Illinois at Urbana-Champaign, 2012

Urbana, Illinois

Adviser:

Associate Professor Sascha Hilgenfeldt

ABSTRACT

This work aims to describe the response of a hemicylindrical gas bubble pinned to rigid substrate to an imposed oscillatory far field pressure, and subsequently describe the resulting steady flow that results in the fluid in the exterior of such a bubble.

We first derive an analytical expression for the allowable shape oscillations of a two-dimensional bubble pinned to a wall, in the limit of a thin oscillatory boundary layer, based on the boundary conditions at the bubble surface and at the wall. We show that the shape of the bubble oscillations must depend on the Stokes boundary layer thickness, both close to and away from the wall.

We discuss also the implications of the oscillatory flow on the steady streaming. We show that in order to properly describe the steady streaming, the flow must be resolved to obey simultaneously the correct slip velocity at the wall and the correct stresses at the bubble surface, both of which are specified by the exact shape of the bubble. We evaluate the steady streaming flow by means of an eigenfunction expansion, and compare the results to experimental observations.

Finally, we examine the dynamics of a pinned bubble in response to an imposed oscillatory pressure by a balance of dynamic stresses across the interface. We propose a mechanism by which surface modes may be linearly coupled to the volume oscillations of a pinned bubble, which is otherwise absent for a bubble oscillating in bulk fluid. We compare the frequency responses of the oscillation mode amplitudes and phases to experimental data.

ACKNOWLEDGMENTS

I wish to express my utmost gratitude to my advisor, Sascha Hilgenfeldt, for being a constant source of inspiration and in the absence of whose guidance, this work would have been impossible. Thanks also to Professors West and Matalon, interactions with whom have been most enjoyable and have had direct bearing on this work.

Special thanks to Cheng Wang, whose experimental work has been crucial in the development of the theory presented here, and to Shreyas Jalikop, for his guidance during the initial stages of this work. I also wish to thank my friend Hari for the numerous discussions on fluid mechanics, and on life.

And finally, many warm thanks go out to my family back home for their unconditional love and support.

TABLE OF CONTENTS

CHAPTER 1

INTRODUCTION

1.1 Introduction

Recent years have seen microbubbles gain immense popularity as manipulators of flows at small scales. Despite their small size, they are able to produce surprisingly strong flows and therefore find employment in a variety of scenarios, where they have been used as particle sorters and fluid mixers among a number of other applications [1, 2, 3].

An important mechanism of flow manipulation is acoustic streaming. Streaming is a phenomenon wherein an oscillating fluid near a surface induces, by means of non-linearities, a steady motion of the fluid. The phenomenon is driven by non-vanishing steady viscous stresses that originate close to solid boundaries, which then produce a steady flow near the boundary in question. While the stresses that induce the motion themselves are confined to a small region near the surface, their effect is not, and therefore the entire bulk of the fluid is driven. While the steady flow produced by this mechanism is typically weaker than the oscillatory flow, it tends to be rather powerful at small scales.

The classically studied streaming problem is that of streaming induced by an oscillating rigid cylinder in bulk fluid. While the exact solutions to the problem were described in the 1950s [4, 5], they involved integrals that were in general difficult to evaluate analytically. The asymptotic solutions that were subsequently developed in the limit of a thin oscillatory shear layer [6, 7] were unable to capture important features of the flow [8]. Improvements may be made, however, by employing higher order asymptotics.

The problem of our particular interest is that of a single oscillating bubble attached to a rigid surface, a situation which is desirable for the controlled utilization of bubbles as flow actuators. Oscillating pinned bubbles have

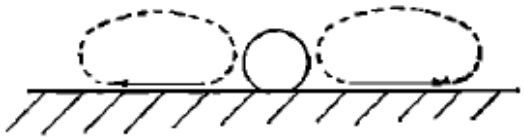

Figure 1.1: Schematic of possible far field streaming due to a compact oscillatory source near a rigid wall, reproduced from Nyborg [10].

successfully been used for a variety of applications such as fluid transport and mixing [1], size sorting of micro particles [3] and the rupture of cells and vesicles [2]. From the point of view of application, it is particularly useful to construct cylindrical bubbles of high aspect ratio, which, for all practical purposes, produces a planar flow that is much easier to control and manipulate as compared to the axisymmetric flow produced by a spherical bubble.

Although bubble streaming is a well-known phenomenon, a deeper understanding of its nature is less so, partly because of the complex nature of bubble oscillations. The streaming flow around a spherical bubble in an unbounded fluid has been described by Longuet-Higgins [9], but the effect of the presence of a wall on the streaming is not fully understood. In his 1958 paper, Nyborg [10] provides a theoretical description of the induced steady slip velocity at the edge of the wall boundary layer produced by an oscillatory point source, and qualitatively suggests the possible flow pattern in the bulk of the fluid, if the oscillatory flow is produced by the oscillating surface of a compact object. We will develop here a theoretical treatment that consistently reconciles the conditions at the bubble with those at the wall.

In Chapter 2, we introduce streaming theory from first principles, which relies on a knowledge of the oscillatory flow in the domain. We revisit Nyborg's problem for the streaming produced by an arbitrary oscillatory flow near a wall. We recognize then, that the oscillatory flow must itself be produced by the bubble and thereby derive a general expression for the oscillatory bubble shapes capable of producing no slip oscillatory flows.

We then use the generalized bubble shape to calculate the streaming near the bubble surface, and then attempt to describe the steady flow in the bulk of the fluid by a set of Stokes solutions that satisfy the appropriate conditions both at the bubble surface and at the wall. The analysis of the steady flow is carried out by means of an eigenfunction expansion consisting of no-slip

Stokes solutions and other Stokes solutions that satisfy the prescribed slip velocity at the edge of the wall boundary layer. We compare the results of the analysis to some experimental results and comment on the efficacy of the theory presented.

We must recognize that the shape of the bubble is ultimately determined by the dynamics of oscillation of the bubble. In Chapter 3, we consider the problem of an oscillating cylindrical bubble pinned to a wall, and describe the oscillatory flow using a potential flow approximation. Here we use also the result from Chapter 2 that the pinning of the bubble to the wall is a boundary layer effect. By means of a dynamic balance of normal stresses across the interface, we describe a method of linearly coupling the volume oscillations to the surface mode dynamics. This coupling depends only on the shape of the bubble at rest, and allows the sustained oscillation of surface modes by the application of a uniform far field pressure. The frequency responses of the different oscillation modes are compared to experimental data.

CHAPTER 2

OSCILLATORY FLOW FIELD AND THE INDUCED STEADY STREAMING

2.1 Introduction

In this chapter, we develop a formal description of the oscillatory flow field and the induced streaming due to an oscillating cylindrical bubble pinned to rigid, no-slip walls. The study of this problem is motivated by the experimental geometry used for particle manipulation used by Wang et al. [3]. The setup typically consists of a micro channel of rectangular cross-section with a side channel in one of its walls. By injecting fluid into the main channel, one may trap a microbubble of the same diameter as the width of the side channel, enclosing a volume of gas within it. The bubble then remains effectively pinned to the main channel by means of two contact lines, as shown in Figure 2.2. Application of ultrasound induces sustained oscillations of the bubble, which then induce steady streaming, both of which are, in general, dependent on the frequency of excitation [11].

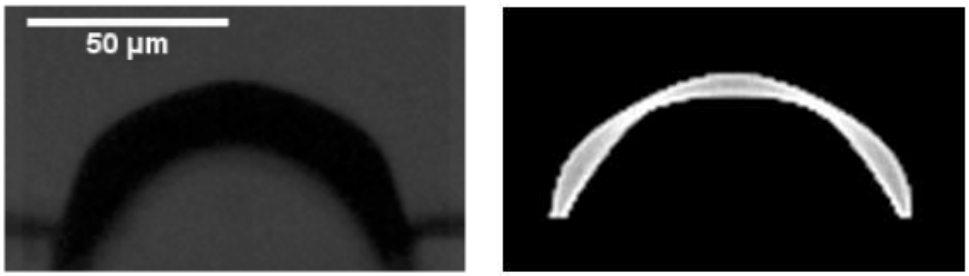

(a) (b)

Figure 2.1: A photograph (a) showing the bubble shape at a particular instant during its oscillation cycle, and a composite image (b) showing extrema of the bubble outline over a cycle of oscillation, reproduced from Wang et al. [11]. The frequency of excitation was 44.6 kHz.

Our objective is to analyze such a system, and determine the dominant features of the induced steady streaming, for any admissible oscillation of the bubble surface.

2.2 Problem definition

Consider a cross section of an infinitely long hemicylindrical bubble of radius a pinned to a rigid surface by means of two contact lines. The surface of the bubble oscillates at an angular frequency ω in a medium of incompressible fluid of uniform density ρ and dynamic viscosity μ, of infinite extent above the rigid surface. If ϵ is the ratio of the amplitude of the bubble oscillation to its radius, we may define a characteristic speed $U = \epsilon a\omega$.

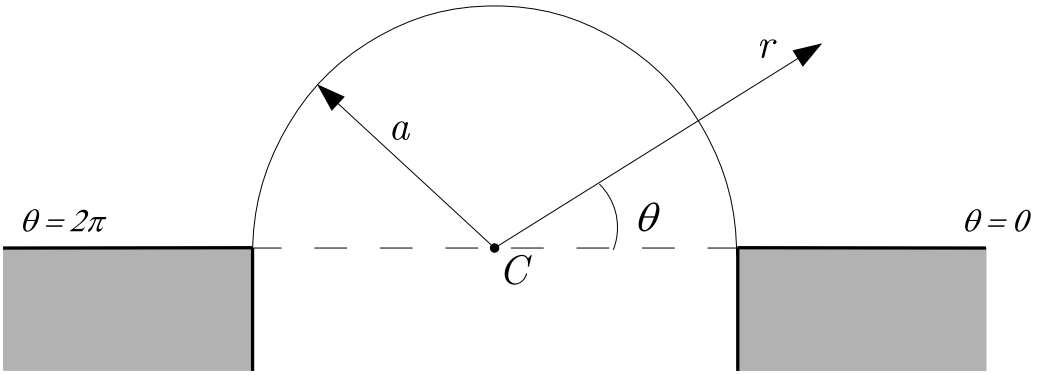

Figure 2.2: Definition of Coordinates for an Oscillating Pinned Bubble

2.3 Streaming theory for a two dimensional flow

The vorticity equation for incompressible flow is

$$\frac{\partial \boldsymbol{\zeta}}{\partial t} + (\boldsymbol{u}.\boldsymbol{\nabla})\boldsymbol{\zeta} - (\boldsymbol{\zeta}.\boldsymbol{\nabla})\boldsymbol{u} = \nu\nabla^2\boldsymbol{\zeta}, \tag{2.1}$$

where $\boldsymbol{u}$ and $\boldsymbol{\zeta}$ are the velocity and the vorticity fields respectively. If the flow is two dimensional, we may rewrite the equation in polar coordinates in terms of a stream function Ψ

$$\frac{\partial \nabla^2\Psi}{\partial t} - \frac{1}{r}\frac{\partial(\Psi, \nabla^2\Psi)}{\partial(r,\theta)} = \nu\nabla^4\Psi, \tag{2.2}$$

where we have used, in the interest of brevity,

$$\frac{\partial(f,g)}{\partial(x,y)} = \frac{\partial f}{\partial x}\frac{\partial g}{\partial y} - \frac{\partial f}{\partial y}\frac{\partial g}{\partial x}.$$

In this notation, the velocity components are given as

$$u_r = \frac{1}{r}\frac{\partial \Psi}{\partial \theta}, \quad u_\theta = -\frac{\partial \Psi}{\partial r}$$

and the vorticity vector $\boldsymbol{\zeta}$ as,

$$\boldsymbol{\zeta} = -\nabla^2 \Psi \; \boldsymbol{e_z}.$$

Using a, ω^{-1} and U as characteristic scales for length, time and velocity respectively, one may define a dimensionless ratio $\epsilon = U/a\omega$, and write the governing equation in the form

$$\frac{\partial \nabla^2 \Psi}{\partial t} - \frac{\epsilon}{r}\frac{\partial(\Psi, \nabla^2\Psi)}{\partial(r,\theta)} = \frac{\delta^2}{2}\nabla^4 \Psi, \tag{2.3}$$

where δ is the dimensionless Stokes boundary layer thickness defined as

$$\delta = \sqrt{\frac{2}{Re}} = \frac{1}{a}\sqrt{\frac{2\nu}{\omega}}.$$

It will be assumed that the Stokes layer thickness δ is much smaller than unity, which is equivalent to assuming that the primary Reynolds number is much greater than unity, for the remainder of the text. If the amplitude of oscillation is much smaller than the size of the bubble ($\epsilon \ll 1$), we may develop an asymptotic solution in ϵ.

$$\Psi(r,\theta,\delta,\epsilon,t) = \Psi_0(r,\theta,\delta,t) + \epsilon\, \Psi_1(r,\theta,\delta,t) + O(\epsilon^2). \tag{2.4}$$

The leading order term in the above expansion represents the flow field produced by the oscillation of the bubble surface. It is therefore also a strictly time periodic function at the same angular frequency ω as that of the bubble oscillation.

$$\left(\frac{\partial}{\partial t} - \frac{\delta^2}{2}\nabla^2\right)\nabla^2 \Psi_0 = 0. \tag{2.5}$$

Note that for small δ, the oscillatory flow is irrotational to leading order, in the bulk of the fluid. The effect of viscosity (and therefore the vorticity) is confined to the viscous shear layer near surfaces of discontinuity.

If one carries out the asymptotic analysis to $O(\epsilon)$, one obtains the governing equation for the stream function Ψ_1 describing the secondary flow,

$$\nabla^4\Psi_1 - \frac{\partial\nabla^2\Psi_1}{\partial t} = -\frac{2}{\delta^2}\frac{1}{r}\frac{\partial(\Psi_0, \nabla^2\Psi_0)}{\partial(r,\theta)}. \tag{2.6}$$

From the nature of the forcing term in Eq.(2.6), it is clear that Ψ_1 may, in general, comprise both time dependent and steady components. Assuming that the time dependence of Ψ_1 has zero mean, the steady component of the secondary flow Ψ_s is given by the time average of Ψ_1. The equation that governs the steady Eulerian streaming is therefore

$$\nabla^4\Psi_s = \langle\Psi_1\rangle = -\frac{2}{\delta^2}\left\langle\frac{1}{r}\frac{\partial(\Psi_0, \nabla^2\Psi_0)}{\partial(r,\theta)}\right\rangle, \tag{2.7}$$

where $\langle.\rangle$ represents a time average over a cycle of oscillation. The non-homogeneous term in Eq.(2.7) is non-zero only in regions of non-zero fluctuating vorticity. It then follows that in the bulk of the fluid, where the oscillatory flow is irrotational, the steady flow represents a Stokes flow. This steady Stokes flow is driven by the Reynolds stresses near discontinuity surfaces, produced as result of a non-zero oscillatory vorticity.

It is natural to define a streaming Reynolds number Re_s, using the characteristic speed of streaming ϵU. It must be noted that the equation that governs the streaming presented here holds only if the streaming Reynolds number is much smaller than unity [12, 13], which is equivalent to the condition $\epsilon \ll \delta$.

The consequences of this condition not being satisfied is that the inertia of the steady flow becomes important and full Navier-Stokes equations must be solved in order to describe it. This has been discussed to some extent separately by Riley [14] and Stuart [15] in the context of an oscillating solid cylinder for $Re_s \gg 1$. For large values of Re_s, a jet-like steady flow coaxial with the direction of oscillation of the cylinder is produced. For the remainder of this text, the inertia of the steady flow will be assumed negligible.

For a cylindrical bubble in bulk fluid, the solution to (2.5) may be found exactly for any given oscillatory deformation of the bubble surface from rest.

This is done by means of a modal decomposition in the angular coordinate θ. Subsequently, the steady streaming in this particular case may also be computed, albeit asymptotically in the limit of a thin boundary layer near the bubble surface. However, in the domain of current interest, an exact solution is not easily found for the oscillatory flow field. Furthermore, the exact shape of the bubble oscillation required to produce a flow that does not slip over the wall is not obvious. Since the viscous stresses near the interfaces ultimately drive the steady streaming, it is crucial to describe the structure of viscous regions accurately everywhere in the domain. We will examine the equation governing the oscillatory flow, Eq.(2.5), in various regions of the domain and construct a uniformly valid asymptotic solution for the flow field. A similar treatment shall be attempted for the steady streaming.

2.4 Flow over a plane no-slip surface

We describe here the general form for the oscillatory flow over a wall and subsequently the induced streaming. To do so, we examine the governing equations in a boundary layer of thickness δ over the wall. A similar treatment may also be found in a 2001 review by Riley [13]. We use a boundary layer coordinate ξ and a boundary layer stream function ϕ defined by

$$\begin{aligned} &\theta = \delta\,\xi, \text{ and} \\ &\Psi(r,\theta,\delta,\epsilon) \to \delta\,\phi(r,\xi,\delta,\epsilon). \end{aligned} \tag{2.8}$$

We will now solve for ϕ by means of an asymptotic expansion that runs in parallel with Eq.(2.4),

$$\phi(r,\xi,\delta,\epsilon,t) = \phi_0(r,\xi,\delta,t) + \epsilon\,\phi_1(r,\xi,\delta,t) + O(\epsilon^2). \tag{2.9}$$

In this region of the domain, we may write

$$\nabla^2 \sim \frac{1}{\delta^2}\frac{1}{r^2}\frac{\partial^2}{\partial\xi^2} + O(1).$$

We seek time periodic solutions of the form $\phi_0(r,\xi)e^{it}$, where it shall be understood that only the real part of any complex quantity is of physical

significance. The governing equations for the near-wall oscillatory flow and the streaming respectively assume the forms

$$\left(\frac{\partial^2}{\partial\xi^2} - 2ir^2\right)\frac{\partial^2}{\partial\xi^2}\phi_0 = 0 + O(\delta^2) \tag{2.10}$$

and

$$\frac{1}{2r^4}\frac{\partial^4\phi_s}{\partial\xi^4} = \left\langle -\frac{1}{r}\frac{\partial\left(\phi_0, \frac{1}{r^2}\frac{\partial^2\phi_0}{\partial\xi^2}\right)}{\partial\left(r,\xi\right)}\right\rangle + O(\delta^2), \tag{2.11}$$

where ϕ_s is the steady component of ϕ_1, and is given by a time-averaging as $\phi_s = \langle\phi_1\rangle$. We also require that the velocity of the fluid at the surface of the wall is zero, and hence we have the boundary conditions

$$\frac{\partial\phi}{\partial\xi} = \frac{\partial\phi}{\partial r} = 0 \text{ at } \xi = 0 \tag{2.12}$$

Suppressing solutions that are unbounded as $\xi \to \infty$, we have for the oscillatory flow, to $O(\delta^2)$

$$\phi_0(r,\xi) = ru(r)\left\{\xi - \frac{1}{r(1+i)}\left(1 - e^{-(1+i)\xi r}\right)\right\}e^{it}, \tag{2.13}$$

where $u(r)$ is the oscillatory slip velocity at the edge of the wall boundary layer and the real part is understood. The solution (2.13) is valid under the condition that the derivatives of the ϕ_0 tangential to the wall are small in comparison to those normal to the wall. It is therefore expected that the above treatment breaks down in the corner region that is a distance of the order of δ both from the wall and from the bubble surface, which we will discuss separately. The form of Eq.(2.13) for large ξ sets the matching condition for the outer flow when $r \sim O(1)$. Thus, we have a matching condition for the oscillatory outer stream function near $\theta = 0$,

$$\psi_0(r,\theta\to 0) \sim \left[ru(r)\theta - \frac{\delta}{(1+i)}u(r)\right]e^{it}. \tag{2.14}$$

The oscillatory wall solution in Eq.(2.13) is now used to calculate the steady streaming in the wall boundary layer. We are specifically interested in the wall streaming that persists beyond the Stokes shear layer, and which thereby affects the bulk of the fluid. The real part of the time averaged

product of two complex quantities of the form Ue^{it} and Ve^{it} is given by $\frac{1}{2}UV^*$, or equivalently by $\frac{1}{2}U^*V$ where the the asterisk implies a complex conjugate [9]. Using the expression for the oscillatory stream function in Eq.(2.13), the equation for the near-wall steady streaming Eq.(2.11) may be written, after simplification, as

$$\begin{aligned}\frac{\partial^4\phi_s}{\partial\xi^4} =& r^4\left\{(1+i)G+(1-i)G^*\right\}\left(e^{-(1+i)r\xi}-e^{-2r\xi}\right)\\ &+2i\,r^5\,G^*\xi e^{-(1+i)r\xi},\end{aligned} \tag{2.15}$$

where

$$G(r)=u^*\frac{\partial u}{\partial r}. \tag{2.16}$$

Integrating Eq.(2.15), with the boundary conditions in Eq.(2.12), we have

$$\phi_s=-\frac{3}{4}(1-i)\,G\,r\xi+\frac{1}{8}\,G\,(13-3i)+\phi_s^{BL}+M\xi^2+N\xi^3. \tag{2.17}$$

M and N are determined ultimately by the outer flow via matching. ϕ_s^{BL} comprises all terms that are confined to the Stokes boundary layer and is given by

$$\begin{aligned}\phi_s^{BL} =& -\frac{1}{8}\left[2e^{-(1+i)r\xi}+\frac{1}{2}e^{-2r\xi}\right]\left[(1+i)G+(1-i)G^*\right]\\ &-i\,G^*e^{-(1+i)r\xi}\left[(1-i)+\frac{1}{2}r\xi\right].\end{aligned}$$

The steady velocity at the edge of the boundary layer is found by examining ϕ_s for large ξ. Notably, the streaming near the wall imposes an $O(1)$ slip velocity and an $O(\delta)$ normal velocity. Consequently, in order to effect proper matching to the wall boundary layer solution, the outer flow near $\theta=0$ and $r\sim O(1)$ must assume the form

$$\psi_s(r,\theta\to 0)\sim-\frac{3}{4}(1-i)\,G\,r\theta+\frac{\delta}{8}G\,(13-3i). \tag{2.18}$$

2.5 Flow produced by a bubble

We must recognize that the flow field is ultimately driven by the motion of the bubble surface. In addition to producing a steady streaming at the edge of the wall boundary layer, the oscillatory bubble boundary layer produces a streaming of its own. The challenge then is to reconcile the steady flow in the bulk of the fluid with the steady boundary layer solutions near both the bubble surface and the wall. In this section we will first examine the family allowed oscillation modes of the bubble, and subsequently derive an expression for the resulting steady streaming.

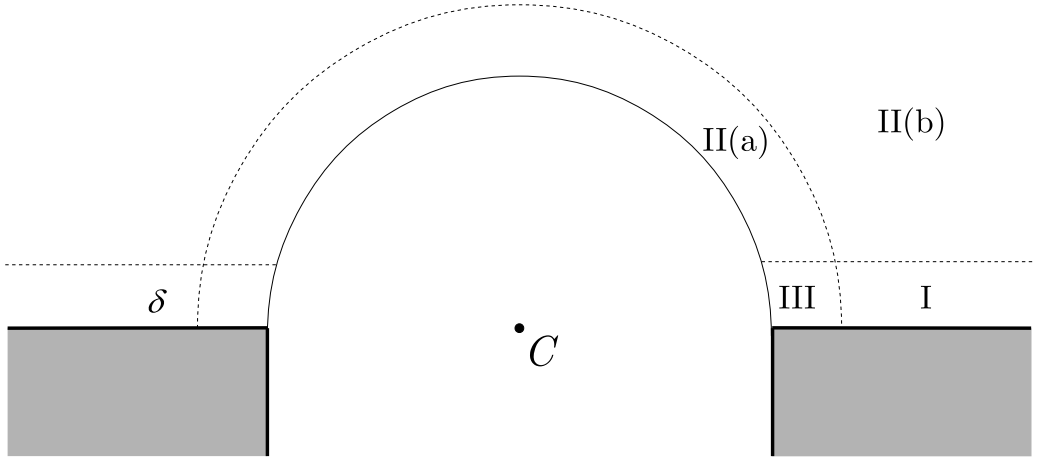

Figure 2.3: Sketch of the different regions of the domain, showing oscillatory viscous boundary layers near discontinuity surfaces. Regions I and III are referred to as the wall boundary layer and the corner region respectively. Regions II(a) and II(b) are collectively termed as the "outer region", which includes the oscillatory shear layer around the bubble.

We consider here a region, henceforth referred to as the "outer region", that excludes the oscillatory wall boundary layer, but includes the viscous shear layer that surrounds the bubble surface, as shown in Figure 2.3. The shape of the part of the bubble in the outer region is henceforth referred to as the "outer bubble shape" and is assumed to have the form

$$R(\theta, t) = 1 - i\,\epsilon\, z(\theta) e^{it}, \tag{2.19}$$

where $z(\theta)$ is in general, a complex valued function and the real part in understood. It must be noted that since the domain under consideration excludes regions that are distances on the order of δ from the wall, one may

not yet impose conditions on $z(\theta)$ near the contact lines. The velocity of the interface normal to itself is calculated as

$$\dot{R}(\theta, t) = \epsilon\, z\,(\theta)\, e^{it}. \tag{2.20}$$

By continuity, the velocity of the fluid normal to the interface must be equal to $\dot{R}$ at the surface of the bubble. It may be assumed that the tangential stress at the surface of the bubble is zero [9]. We define an outer stream function ψ in this region which is developed as an asymptotic series analogous to (2.4), as

$$\psi \sim \psi_0 + \epsilon\psi_1.$$

The governing equation for the oscillatory outer stream function is then

$$\left(\frac{\partial}{\partial t} - \frac{\delta^2}{2}\nabla^2\right)\nabla^2\psi_0 = 0, \tag{2.21}$$

and the steady streaming $\psi_s = \langle\psi_1\rangle$ satisfies

$$\nabla^4\psi_s = -\frac{2}{\delta^2}\left\langle \frac{1}{r}\frac{\partial(\psi_0, \nabla^2\psi_0)}{\partial(r,\theta)}\right\rangle, \tag{2.22}$$

where $\langle . \rangle$ represents a time average over a cycle of oscillation. In addition to the matching conditions at the wall, the outer stream function must satisfy boundary conditions at the bubble interface, given by

$$\left.\begin{aligned} &\frac{1}{r}\frac{\partial\psi}{\partial\theta} = z(\theta)e^{it}, \\ &\frac{\partial^2\psi}{\partial r^2} - \frac{1}{r}\frac{\partial\psi}{\partial r} = 0 \end{aligned}\right\} r = R \tag{2.23}$$

2.5.1 Oscillatory bubble flow

We assume that the oscillatory stream function takes a form $\psi_0(r, \theta, t) = \psi(r, \theta)e^{it}$. We have then for the oscillatory flow

$$\left(\nabla^2 - \alpha^2\right)\nabla^2\psi_0 = 0, \tag{2.24}$$

where α is a complex inverse boundary layer thickness defined as

$$\alpha = \frac{(1+i)}{\delta}.$$

To leading order in ϵ, the boundary conditions at the bubble surface may be applied at $r = 1$ instead of at $r = R$. The kinematic and no-stress boundary conditions for the oscillatory flow are thus

$$\left.\begin{aligned} &\frac{1}{r}\frac{\partial \psi_0}{\partial \theta} = z(\theta)e^{it}, \\ &\frac{\partial^2 \psi_0}{\partial r^2} - \frac{1}{r}\frac{\partial \psi_0}{\partial r} = 0 \end{aligned}\right\} r = 1 \tag{2.25}$$

The general solution to Eq.(2.24) subject to the boundary conditions in Eq.(2.25), with $z(\theta) = i\exp\{ik\theta\}$ is

$$\psi_0^k(r,\theta) = \lambda_k(r,\alpha)\exp\{ik\theta\}e^{it}, \tag{2.26}$$

where

$$\begin{aligned} \lambda_k(r,\alpha) &= \left(\frac{C_k}{r^k} + D_k K_k(\alpha r)\right), \\ D_k &= -\frac{2+k}{\alpha^2 K_{k-2}(\alpha) + 2k\alpha K_{k-1}(\alpha)}, \text{ and} \\ C_k &= \frac{1}{k} - D_k K_k(\alpha), \end{aligned} \tag{2.27}$$

where $K_k(\alpha r)$ represents a modified Bessel function of the second kind, of order k, k being an arbitrary constant. Note that we recover the solution for an oscillatory monopole in the limit $k \to 0$. It is also worthwhile noting that the algebraically decaying term is a potential flow solution, and that the modified Bessel functions decay exponentially for large values of α, constituting the structure of the no-stress bubble boundary layer.

An expansion in a boundary layer coordinate near the bubble surface shows that the bubble boundary layer terms are $O(\delta^2)$ while the wall boundary layer terms found are $O(\delta)$. It is in general true that no-stress shear layers are $O(\delta)$ weaker than no-slip layers, as is case for an oscillating spherical bubble [9]. That said, it would be impossible to capture the no-stress shear layer near

the bubble surface with the order of δ used to describe the wall boundary layer. In the interest of effecting a matching to the wall layer consistently, the $O(\delta^2)$ terms are restricted to the thin shear layer around the bubble.

Far away from both the bubble and the wall ($r \sim O(1)$), the outer flow takes the form

$$\psi_0^k(r \gg \delta, \theta) \sim \frac{1}{kr^k} \exp\{ik\theta\} e^{it} + O(\delta^2), \tag{2.28}$$

and represents a potential flow, as discussed earlier. We require additionally that the solution assumes a form that matches to the oscillatory wall solution in Eq.(2.14)

$$\psi_0(r, \theta \to 0) \sim \left[ru(r)\theta - \frac{\delta}{(1+i)} u(r) \right] e^{it}.$$

Taking into account the symmetric boundary conditions at the wall at $\theta = \pi$, we find that the only allowable potential flows $\tilde{\psi_0}$ that also satisfy the matching conditions at the walls are of the kind

$$\tilde{\psi_0^n}(r, \theta) = \frac{1}{r^n} \left\{ \frac{1}{n} \sin n\theta - \frac{\delta}{(1+i)} \frac{1}{r} \cos(n+1)\theta \right\} e^{it} \tag{2.29}$$

where n is an non-negative integer. The oscillatory slip velocity u_n implied by the potential flow solution in Eq.(2.29) is given as

$$u_n(r) = \frac{1}{r^{n+1}}.$$

It follows from the linearity of the governing equation and the boundary conditions for the oscillatory flow, that the outer flow, inclusive of the boundary layer near the bubble may be expressed as a linear combination of the form

$$\psi_0 = \sum_n A_n e^{i\phi_n} \left[\lambda_n(r, \alpha) \sin n\theta - \delta \frac{n+1}{1+i} \lambda_{n+1}(r, \alpha) \cos(n+1)\theta \right] e^{it}, \tag{2.30}$$

where A_n and ϕ_n are respectively the amplitude and phase of the nth oscillation mode. We will confine, without loss of generality, A_n to the set of non-negative real numbers and ϕ_n to the domain $[0, 2\pi)$. The corresponding

oscillatory slip velocity over the wall boundary layer is then given as

$$u(r) = \sum_n A_n e^{i\phi_n} \frac{1}{r^{n+1}}. \tag{2.31}$$

The shape of the bubble surface outside the viscous region near the wall is then given by the kinematic boundary condition in Eq.(2.25) as

$$\begin{aligned} z(\theta) &= \frac{1}{r}\frac{\partial \psi_0}{\partial \theta}\Big|_{r=1} \\ &= \sum_n A_n e^{i\phi_n} \left[\cos n\theta + \delta \, \frac{n+1}{1+i} \sin{(n+1)\theta}\right]. \end{aligned} \tag{2.32}$$

2.5.2 Oscillatory Flow in the Corner

Before we proceed to the treatment of the streaming produced by the bubble boundary layer and the eventual matching with the apparent steady slip at the wall, we examine the oscillatory flow in the corner region near ($r = 1, \theta = 0$). We assume that the wall is no-slip in this region and lines of contact between the bubble and the interface is stationary. We use rescaled variables in the corner

$$\begin{gathered} r = 1 + \eta\delta, \\ \theta = \eta\xi, \text{ and} \\ \Psi(r, \theta, \delta, \epsilon) \to \delta\chi(\eta, \xi, \delta, \epsilon), \end{gathered}$$

where χ is a rescaled stream function corresponding to the corner flow. In harmony with the asymptotic expansion of Ψ in Eq.(2.4), we express χ as

$$\chi(\eta, \xi, \delta, \epsilon) \sim \chi_0(\eta, \xi, \delta) + \epsilon\chi_1(\eta, \xi, \delta). \tag{2.33}$$

To leading order, we have for the leading order oscillatory stream function in the corner

$$\left(\nabla^2 - \alpha^2\right) \nabla^2 \chi_0 = 0, \tag{2.34}$$

with no slip boundary conditions at the wall

$$\frac{\partial \chi_0}{\partial \xi} = \frac{\partial \chi_0}{\partial \eta} = 0 \text{ at } \xi = 0 \tag{2.35}$$

In addition, we must match both to the wall boundary layer solution as $\eta \to \infty$, and to the bubble boundary layer solution as $\xi \to \infty$. The matching conditions for χ_0 are formally written as

$$\begin{aligned} &\delta\chi_0(\eta, \xi \to \infty) \sim \psi_0(r \to 1, \theta \to 0), \text{ and} \\ &\chi_0(\eta \to \infty, \xi) \sim \phi_0(r \to 1, \xi). \end{aligned} \tag{2.36}$$

From the earlier discussion on the strength of the bubble boundary layer, we expect a $O(\delta)$ weaker contribution from the bubble boundary layer. The outer flow near the corner, to leading order, has the form

$$\psi_0(r \to 1, \theta \to 0) \sim \delta u(1) \left\{ \xi - \frac{1}{1+i} \right\}. \tag{2.37}$$

Note that to this order, we are unable to capture the bubble boundary later terms. The wall boundary layer solution near the corner, expanded to leading order is

$$\phi_0(r \to 1, \xi) \sim u(1) \left\{ \xi - \frac{1}{1+i}(1 - e^{-(1+i)\xi}) \right\}. \tag{2.38}$$

It is easily shown that the leading order solution of χ_0 that is no slip on the wall and satisfies the correct matching conditions is given by

$$\chi_0(1, \xi) \sim u(1) \left\{ \xi - \frac{1}{1+i}(1 - e^{-(1+i)\xi}) \right\}. \tag{2.39}$$

The potential flow solutions, which are exact solutions of the Navier Stokes equations match identically in the corner layer to the same order of matching that carried out far away from the corner. It is worth mentioning that that in order for the bubble surface in the corner region to be no-stress, one must carry out a higher order asymptotic scheme that includes the bubble boundary layer terms. However, the kinematic boundary condition at the surface of the bubble still holds.

Now that we have asymptotically correct oscillatory solutions in the various regions of the domain, a uniformly valid solution accurate to $O(\delta)$ may be constructed and has the form

$$\begin{aligned} \Psi_0(r, \theta) =& \psi_0(r, \theta) \\ &+ \frac{1}{\alpha} \sum_n \frac{A_n e^{i\phi_n}}{r^{n+1}} \left(e^{-\alpha\theta r} + (-1)^{n+1} e^{-\alpha(\pi-\theta)r} \right) e^{it}. \end{aligned} \tag{2.40}$$

It follows that the uniformly valid bubble shape required to produce such an oscillatory flowfield is then

$$\begin{aligned}\mathcal{R}(\theta,t) =& 1 - i\epsilon \left.\frac{\partial \Psi_0}{\partial \theta}\right|_{r=1} \\ =& 1 - i\epsilon \mathcal{Z}(\theta) e^{it},\end{aligned} \tag{2.41}$$

where the form of the shape oscillation $\mathcal{Z}$ may be evaluated as

$$\begin{aligned}\mathcal{Z}(\theta) =& \sum_n A_n e^{i\phi_n} \left[\cos n\theta + \frac{n+1}{\alpha} \sin{(n+1)\theta}\right] \\ &- \sum_n A_n e^{i\phi_n} \left(e^{-\alpha\theta} + (-1)^n e^{-\alpha(\pi-\theta)}\right).\end{aligned} \tag{2.42}$$

The solution for the oscillatory stream function in Eq.(2.40) captures the viscous regions over the wall, around the bubble, and in the corner, along with the oscillatory potential flow in the bulk of the fluid. Additionally, the no-slip condition is satisfied everywhere along the the wall with an exponentially small error for $\delta \ll 1$. At the bubble surface, while the kinematic boundary condition is satisfied exactly, the no-stress boundary condition is only satisfied by the outer flow and breaks down near the contact line. This may may be remedied by using a higher order expansion in δ, which demands a more rigorous treatment of the corner region.

Note that the oscillatory bubble shape in Eq.(2.42) contains features that decay exponentially over distances of the order of δ near the wall, as well as a dependence on δ of the bubble shape away from the wall. Observe also that we have at no point imposed that the outer shape of the bubble be stationary near the walls. The pinning of the bubble in this case is a natural consequence of having a strictly no-slip wall, and is therefore entirely a boundary layer effect. Qualitatively, the theory is in agreement with experimentally observed bubble shape oscillations at large frequencies, particularly near the wall. However, limitations on spatial and temporal resolution of the near-wall bubble shape at large frequencies renders a direct comparision between experiment and theory difficult.

2.5.3 Bubble streaming

We have already described the steaming flow produced in the wall boundary layer; now we shall focus on the streaming induced by the oscillatory shear layer around the bubble. To do so, we may expand the operators and the oscillatory flow in a boundary layer coordinate near the mean surface of the bubble. However, in order to apply the no stress condition at the bubble surface, a solution accurate to $O(\delta^2)$ is required, which makes both the expansion of the streaming equation and its solution tedious. Instead, we shall try and express the inhomogeneity as a linear combination of eigenfunctions of the biharmonic operator.

Recall the equation (2.22) governing the steady streaming in the outer region

$$\nabla^4 \psi_s = -\frac{2}{\delta^2} \left\langle \frac{1}{r} \frac{\partial(\psi_0, \nabla^2 \psi_0)}{\partial(r,\theta)} \right\rangle, \tag{2.43}$$

where $\psi_s = \langle \psi_1 \rangle$ is the steady component of the secondary outer flow. We emphasize again that by "outer flow" and "outer region", we imply the entire region of the domain that excludes the wall boundary layer, but includes the shear layer around the bubble. We relabel the steady stream function ψ_s to ψ^E, since it represents a steady Eulerian stream function.

To construct the right hand side of Eq.(2.43), we use the leading order term of oscillatory outer solution presented in Eq.(2.30), namely a decomposition of the flow field into Fourier modes in the azimuthal direction such that there exists a finite oscillatory slip velocity everywhere along the wall, and zero velocity normal to the wall. This is also reflected in the bubble shape in Eq(2.32), of which only the leading order is retained. We then have

$$\psi_0 = \sum_n \psi_0^n = \sum_n A_n e^{i\phi_n} \lambda_n(r,\alpha) \sin n\theta \, e^{it} \tag{2.44}$$

and

$$z(\theta) = \sum_n A_n e^{i\phi_n} \cos n\theta. \tag{2.45}$$

One may define a mode of the steady streaming ${}_m\psi_n^E$, constructed by two modes of the oscillatory stream function ψ_0^m and ψ_0^n as

$$\nabla^4 \left\{ {}_m\psi_n^E \right\} = -\frac{2}{\delta^2} \left\langle \frac{1}{r} \frac{\partial(\psi_0^m, \nabla^2 \psi_0^n)}{\partial(r,\theta)} \right\rangle. \tag{2.46}$$

Note that ${}_m\psi_n^E$ represents an ordered pair of oscillatory modes ψ_0^m and ψ_0^n. The oscillatory vorticity on the right hand side of Eq.(2.46) decays exponentially away from the bubble surface over a length scale on the order of the Stokes boundary layer thickness. Consequently, the steady forcing term also decays in a similar manner, and hence we attempt to find exponentially decaying eigenfunctions of the biharmonic operator. The eigenvalue problem

$$\nabla^4\psi - \lambda^4\psi = 0 \tag{2.47}$$

admits exponentially decaying eigenfunctions of the form

$$\psi_\nu = K_\nu(\lambda r)\sin\nu\theta \tag{2.48}$$

that decay as $e^{-\lambda r}$ for $\lambda \gg 1$. However, an orthogonal projection of the inhomogeneity onto the space of these eigenfunctions is in general not simple to carry out analytically. It will suffice for the purpose of this discussion that we perform a decomposition that is asymptotically correct to the required order in δ, in order to capture the structure of the boundary layer to sufficient accuracy. It follows that the solution thus obtained is also accurate to the same number of orders in δ. A detailed description of the decomposition of the inhomogeneity into appropriate eigenfunctions, and the subsequent method of solution is provided in Appendix A.1.

The Eulerian stream function, given by the solution to Eq.(2.46) may, in general, be expressed as a sum of a particular solution ${}_m\psi_n^P$ and a homogeneous solution ψ_H

$${}_m\psi_n^E = {}_m\psi_n^P + \psi_H, \tag{2.49}$$

where ${}_m\psi_n^P$ is given by

$$\begin{aligned}
{}_m\psi_n^P =& A_m A_n \left[-\frac{\delta}{4}(1+i)(2+n)e^{-(1+i)\eta} \right. \\
&\left. + \frac{\delta^2}{8}(2+n)\left\{11+8m+(1+i)(3+2m)\eta\right\}e^{-(1+i)\eta} \right] \\
&\qquad e^{i\phi_{nm}}\sin n\theta\cos n\theta \\
&+ A_m A_n \frac{\delta^2}{4} n(2+n)e^{-(1+i)\eta}e^{i\phi_{nm}}\sin m\theta\,\cos n\theta.
\end{aligned} \tag{2.50}$$

$\eta = (r-1)/\delta$ is a boundary layer coordinate defined positive outward from

the bubble surface, as defined in Subsection 2.5.2, and $\phi_{mn} = \phi_m - \phi_n$ is the phase difference between the two modes. The homogeneous solution ψ_H is a linear combination of Stokes solutions and satisfies $\nabla^4 \psi_H = 0$. Note that since ${}_m\psi_n^P$ is exponentially decaying, the Eulerian mean flow in the bulk of the fluid is ultimately constituted by Stokes solutions, which are also required in order to satisfy the boundary conditions at the bubble surface and at the wall.

In order to compare our results to the steady motion of material points in the fluid, we compute the Lagrangian steady streaming. The Lagrangian mean flow is obtained by adding a Stokes drift stream function ψ^d to the Eulerian steady streaming.

$$\psi^L = \psi^E + \psi^d \tag{2.51}$$

The Stokes drift velocity is in general given by

$$\boldsymbol{u}_d = \left\langle \left(\int \boldsymbol{u} dt . \nabla \right) \boldsymbol{u} \right\rangle,$$

where $\boldsymbol{u}_d$ is the Stokes drift velocity field. This may be translated into a Stokes drift stream function [16], using the formalism for time averaging described earlier, as

$$\psi^d = \frac{1}{r} \left\langle -i \frac{\partial \psi_0}{\partial \theta} \frac{\partial \psi_0}{\partial r} \right\rangle = \frac{i}{2r} \left[\frac{\partial \psi_0}{\partial r} \frac{\partial \psi_0^*}{\partial \theta} \right]. \tag{2.52}$$

Note here that the Stokes drift may contain long range algebraically decaying terms as well as exponentially decaying ones that are confined to the bubble boundary layer. Longuet-Higgins showed that for an oscillating spherical bubble in bulk fluid, the induced streaming is strongest between distinct pairs of modes, due to contributions from the Stokes drift [9]. For any two modes of the oscillatory stream function ψ_0^m and ψ_0^n, we define a Stokes drift term ${}_m\psi_n^d$ such that

$${}_m\psi_n^d = \frac{i}{2r} \left[\frac{\partial \psi_0^m}{\partial r} \frac{\partial \psi_0^{n*}}{\partial \theta} \right]. \tag{2.53}$$

The Stokes drift is evaluated to leading order in the long-range decay term and to $O(\delta^2)$ in the steady boundary layer terms, in order to capture the leading order the velocity contribution to the bulk of the fluid and the leading

order tangential stress at the mean bubble surface. We then have

$$
\begin{aligned}
{}_m\psi_n^d =& A_m A_n \left[-\frac{i}{2}\frac{1}{r^{m+n+2}} + \frac{\delta}{4}(1+i)(2+n)e^{-(1+i)\eta} \right. \\
& \left. - \frac{\delta^2}{8}(2+n)\left\{3+(1+i)(3+2m)\eta\right\}e^{-(1+i)\eta} \right] \\
& \qquad e^{i\phi_{nm}}\sin n\theta\cos m\theta \\
& - A_m A_n \frac{\delta^2}{4} m(2+m)e^{-(1+i)\eta}e^{-i\phi_{nm}}\sin n\theta\,\cos m\theta. \qquad (2.54)
\end{aligned}
$$

The Eulerian streaming and Stokes drift stream functions resulting from the pair of oscillation modes m and n are then given by $\psi_{mn}^E = {}_m\psi_n^E + {}_n\psi_m^E$ and $\psi_{mn}^d = {}_m\psi_n^d + {}_n\psi_m^d$ respectively. We are now in a position to compute the Lagrangian streaming $\psi_{mn}^L = \psi_{mn}^E + \psi_{mn}^d$, for any given pair of oscillation modes m and n. The Lagrangian streaming may be written as

$$
\psi_{mn}^L = 2\hat{\psi}_{mn} + \psi_H, \qquad (2.55)
$$

where $\hat{\psi}_{mn}$ is given by

$$
\begin{aligned}
\hat{\psi}_{mn} =& A_m A_n \left[\frac{1}{4}\frac{1}{r^{m+n+2}}\sin\phi_{mn}\sin(m-n)\theta \right. \\
& + \frac{\delta^2}{2}(2+n)(1+m)e^{-(1+i)\eta}\,e^{-i\phi_{mn}}\sin n\theta\cos m\theta \\
& \left. + \frac{\delta^2}{2}(2+m)(1+n)e^{-(1+i)\eta}\,e^{i\phi_{mn}}\sin m\theta\cos n\theta \right]. \qquad (2.56)
\end{aligned}
$$

Note that all the quantities that may be directly evaluated from the oscillatory flow, namely, the bubble boundary layer terms and the Stokes drift, are contained within $\hat{\psi}_{mn}$. Notice also the negation of the leading order boundary term of the Eulerian streaming by the Stokes drift. One must note that in principle, one may calculate Stokes drift contributions in the wall boundary layer as well. However, the only additional Stokes drift terms decay exponentially away from the wall over a length scale of the order of the Stokes layer thickness δ and therefore have no effect on the flow in the bulk.

2.5.4 Steady Flow in the Bulk

The Lagrangian stream function for the entire flow-field may be written as a sum over pairs (m,n) of ψ^L_{mn}, with the exception that for $m = n$, the expression in Eq.(2.56) must be halved. This is written as

$$\psi^L = \psi_H + \hat{\psi}, \tag{2.57}$$

where $\hat{\psi} = \sum_n \sum_m \hat{\psi}_{mn}$, and we have used a double sum over indices m and n in favour of the sum over pairs (m,n).

The steady homogeneous solution ψ_H is determined from the boundary conditions imposed at the bubble surface and the matching conditions imposed at the edge of the wall boundary layer. We show in Appendix A.2 that the Lagrangian mean flow ψ^L is no-penetration and no-stress at the mean position of the bubble. The boundary conditions at the surface of the bubble for the Lagrangian mean flow may be formally written as

$$\left.\begin{aligned} &\frac{1}{r}\frac{\partial \psi^L}{\partial \theta} = 0, \\ &\frac{\partial^2 \psi^L}{\partial r^2} - \frac{1}{r}\frac{\partial \psi^L}{\partial r} = 0 \end{aligned}\right\} r = 1 \tag{2.58}$$

In order to calculate the steady slip velocity at the edge of the wall boundary layer, we employ the result from Eq.(2.18), for which we are first required to compute the oscillatory slip velocity. The oscillatory slip velocity at the edge of the wall boundary layer $u_m(r)$ for a mode ψ_m of the oscillatory outer stream function ψ_0 is given by

$$u_m(r) = A_m e^{i\phi_m} \frac{1}{r^{m+1}} e^{it}. \tag{2.59}$$

We define a function ${}_mG_n(r)$, a mode of the quantity $G(r)$ in Eq.(2.16) as

$$\begin{aligned} G_{m,n} &= u_m^* \frac{\partial u_n}{\partial r} \\ &= -(n+1)\frac{A_m A_n}{r^{m+n+3}} e^{-i\phi_{mn}}. \end{aligned} \tag{2.60}$$

The contribution to $G(r)$ by a pair of oscillation modes (m,n) is then given by $G_{mn} = {}_mG_n + {}_nG_m$. The steady Eulerian slip velocity U^E_{mn} at the edge of

the wall boundary layer for a pair of modes (m, n) may then be calculated, using Eq.(2.18) as

$$\begin{aligned} U^E_{mn} &= -\frac{3}{4}(1-i)G_{mn} \\ &= \frac{3}{4}\frac{A_m A_n}{r^{m+n+3}}\Big[(m+n+2)\cos\phi_{mn} + (m-n)\sin\phi_{mn}\Big]. \end{aligned} \tag{2.61}$$

It follows that the steady slip velocity over the wall boundary layer imposed by the entire oscillatory flow field is simply a sum of the contributions from each pair of modes (m, n), which is written instead as a double summation over the indices m and n. We then have

$$U^E = \sum_n \sum_m \frac{U^E_{mn}}{2}. \tag{2.62}$$

To leading order, the steady velocity of the bulk of the fluid normal to the wall is zero, as implied by Eq.(2.12). The Stokes solutions constitute the steady flow in the bulk of the fluid, with the boundary conditions imposed both at the bubble surface and at the wall. We have

$$\nabla^4 \psi_H = 0, \tag{2.63}$$

with the boundary conditions

$$\left.\begin{aligned} &\frac{\partial \psi_H}{\partial \theta} = -\frac{\partial \hat{\psi}}{\partial \theta}, \\ &\frac{\partial^2 \psi_H}{\partial r^2} - \frac{1}{r}\frac{\partial \psi_H}{\partial r} = -\frac{\partial^2 \hat{\psi}}{\partial r^2} + \frac{1}{r}\frac{\partial \hat{\psi}}{\partial r} \end{aligned}\right\} r = 1;\ 0 < \theta < \pi \tag{2.64}$$

and

$$\left.\begin{aligned} &\frac{1}{r}\frac{\partial \psi_H}{\partial \theta} = U^E, \\ &\frac{\partial \psi_H}{\partial r} = 0 \end{aligned}\right\} \theta = 0, \pi;\ r > 1 \tag{2.65}$$

In addition, we must also impose the condition that the steady fluid velocity is bounded as $r \to \infty$. To accommodate the boundary conditions at the wall, we write the solution to Eq.(2.63) as a combination of 'no-slip solutions' and

'slip solutions', where we will impose the slip velocity at the edge of the wall boundary layer. In general, we may write

$$\begin{aligned}\psi_H = &\sum_k \frac{E_k}{r^k}\left[\cos k\theta - \cos(k+2)\theta\right] \\ &+ \sum_k \frac{F_k}{r^k}\left[\frac{1}{k}\sin k\theta - \frac{1}{k+2}\sin(k+2)\theta\right] \\ &+ \sum_n \sum_m \frac{3}{8}\frac{1}{r^{m+n+2}}\gamma_{mn}\sin(m+n+2)\theta, \end{aligned} \tag{2.66}$$

where k is any non-negative integer and

$$\gamma_{mn} = A_m A_n \left[\cos\phi_{mn} + \frac{m-n}{m+n+2}\sin\phi_{mn}\right]. \tag{2.67}$$

The first two series in Eq.(2.66) are no-slip Stokes solutions, and the third series comprises slip-solutions. The boundary matching conditions at the wall are now satisfied identically, and the coefficients E_k and F_k are determined by the boundary conditions at the surface of the bubble.

Note that the two families of no-slip Stokes solutions presented in Eq.(2.66) are not linearly independent functions of the azimuthal coordinate θ. Consequently the boundary conditions at the mean bubble surface are projected onto an orthogonal basis in order to obtain algebraic equations for the coefficients E_k and F_k. We may then write the boundary conditions as

$$\left.\begin{aligned} &\frac{\partial}{\partial\theta}\left\langle \psi_H, \cos n\theta \right\rangle = -\frac{\partial}{\partial\theta}\left\langle \hat{\psi}, \cos n\theta \right\rangle, \\ &\left\langle \frac{\partial^2\psi_S}{\partial r^2} - \frac{1}{r}\frac{\partial\psi_H}{\partial r}, \cos n\theta \right\rangle = \left\langle -\frac{\partial^2\hat{\psi}}{\partial r^2} + \frac{1}{r}\frac{\partial\hat{\psi}}{\partial r}, \cos n\theta \right\rangle \end{aligned}\right\} r = 1; \tag{2.68}$$

where n is a positive integer and $\langle . \rangle$ is an inner product defined as

$$\langle f(\theta), g(\theta)\rangle = \int_0^\pi f(\theta)g(\theta)\,d\theta$$

The evaluation of the boundary conditions (2.68) for different values of n yields a coupled system of linear equations in E_k and F_k. Note that the the system, in theory, is infinite in extent, even for a finite number of oscillation

modes of the bubble.

2.6 Results and discussion

Here we discuss the steady flow produced by a bubble that executes, to leading order, purely volumetric oscillations. In such a case, the surface of the bubble itself induces no streaming. Nevertheless, a steady slip velocity is implied over the wall boundary layer, resulting from Reynolds stresses in the Stokes boundary layer over the wall. It follows from the shape of the oscillation that there is are no contributions to Stokes drift that persist in the bulk of the fluid, and therefore, the flow in the bulk is governed by a biharmonic Eulerian stream function that satisfies the boundary conditions

$$\left.\begin{aligned} &\frac{\partial \psi_H}{\partial \theta} = 0, \\ &\frac{\partial^2 \psi_S}{\partial r^2} - \frac{1}{r}\frac{\partial \psi_H}{\partial r} = 0 \end{aligned}\right\} r = 1;\ 0 < \theta < \pi \tag{2.69}$$

and

$$\left.\begin{aligned} &\frac{1}{r}\frac{\partial \psi_H}{\partial \theta} = \frac{3}{4r^3}, \\ &\frac{\partial \psi_H}{\partial r} = 0 \end{aligned}\right\} \theta = 0, \pi;\ r > 1 \tag{2.70}$$

where we have normalized by A_0^2, which is now the only relevant amplitude of the streaming flow. Note that this is exactly Nyborg's problem of the streaming flow along a wall produced by an oscillating source. While Nyborg does not consider the structure of the flow near the compact object that produces the oscillatory flow, we may do so using the eigen function decomposition presented earlier. This case is relevant to driving the bubble at frequencies that are typically larger than the resonance frequencies of its first few oscillation modes, we we shall elaborate upon in Chapter 3.

This streamline portrait for the case of a purely radial oscillation is easily reconciled with Nyborg's theory for streaming flow near a wall [10] in that the bulk of the fluid displays a steady flow that seems to be driven by the apparent steady slip over the wall. Fluid is driven towards the bubble at its apex, and away from the bubble along the walls by what we call "anti-

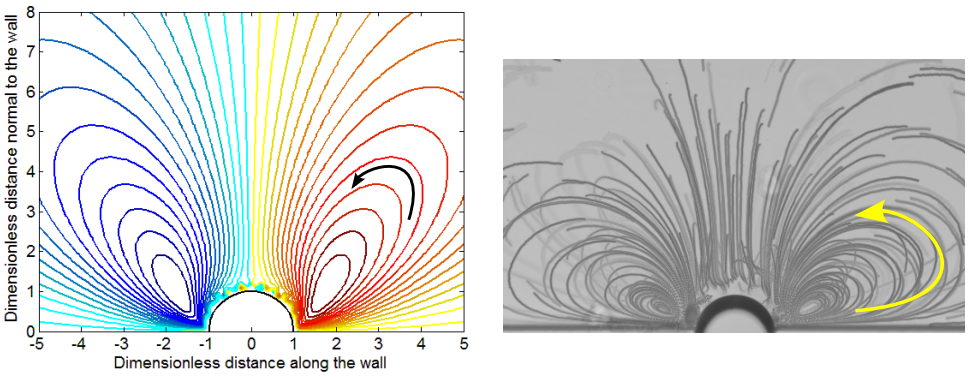

(a) Theory (b) Experiment

Figure 2.4: Theoretical (a) steady streaming flow patterns produced by a oscillating monopole near a wall. This case corresponds to experimental bubble shape data collected at an oscillation frequency of 111 kHz. The experimental steady streaming pattern for this frequency is shown in (b). The arrows represent the direction of flow.

fountain loops", as indicated in Figure 2.4. Note that while the Lagrangian stream function decays as $\psi^L \sim 3/4r^{-2}$ along the wall, we find that away from the wall, the far field decay of the stream function is $\psi^L \sim 3/(5\pi)r^{-1}$, corresponding to a r^{-2} velocity decay. The bulk of the fluid comprises more slowly decaying velocities, which are in general, produced by the most slowly decaying Stokes solution. This is in contrast with the case of a bubble oscillating in bulk, where the exponent of the radial decay of the velocity field depends on the shape of the bubble oscillation, elucidated for axisymmetric oscillations of spherical bubbles by Longuet-Higgins [9]. We have thus solved Nyborg's open problem for the streaming flow produced by an oscillatory source near a wall, by not only considering the steady slip velocity along the wall, but also resolving the streaming flow close to the compact object, in this case the bubble, that drives the oscillatory flow. While our analysis is valid for a two-dimensional flow, it is easily extended to the case of an axisymmetric flow.

An extension of the method to shapes of the bubble oscillation that induce steady streaming at the edge of the bubble boundary layer is possible within the framework we have presented. In experiment, we observe a characteristic change in the direction of streaming when the bubble oscillation has significant contributions from surface modes. However, the theoretical flow field is dominated by the wall streaming, despite the inclusion of features on the

bubble surface capable of driving their own streaming, as is illustrated in Figure 2.5.

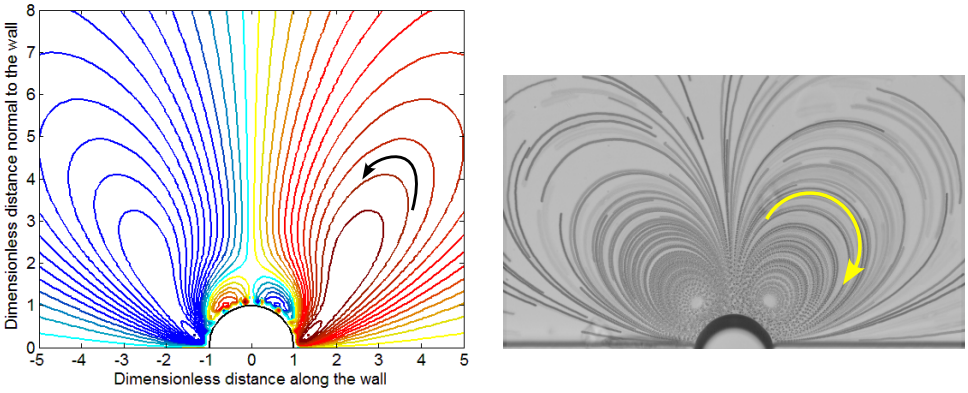

(a) Theory (b) Experiment

Figure 2.5: Theoretical (a) steady streaming flow patterns produced by a combination of oscillating monopole and quadrupole components. Streamlines for the theory are calculated using amplitudes and the phase angles ($A_0 = 1$, $\phi_0 = 0$, $A_2 = 0.7$ and $\phi_2 = \pi/2$) that correspond to experimental bubble shape data collected at a driving frequency of 11.6 kHz. The experimental steady streaming pattern for this frequency is shown in (b). The arrows are representative of the direction of flow.

Note that although the flow is dominated by the anti-fountain loops that are driven by the wall streaming, the theory does show the presence of "fountain loops" near the apex of the bubble. This is in contrast with the experimental observation, namely that the bulk of the fluid is dominated by fountain loops. Experimental observations of the flowfield show that as the frequency of oscillation is increased, the prevailing fountain loops are gradually overcome by anti-fountain loops that originate at the wall. We hope to capture this effect in the theory by the inclusion of higher order asymptotics to better describe the steady boundary structure near the surface of the bubble.

2.7 Concluding remarks

In this chapter, we developed a theory to describe the oscillatory flow and the subsequent streaming flow produced due to an oscillating bubble pinned to a wall. In doing so, we obtained a form for the allowable oscillations of the

bubble surface in the domain, and showed that pinning of the contact line to the wall is a consequence of viscous stresses near the wall. We show also that the shape of the bubble itself is a function of the dimensionless Stokes layer thickness δ, as given in Eq.(2.42). The modification of the classical leading order multipole representation of the bubble shape [17] by δ is two fold. First, the shape of the bubble near the contact line shows an $O(1)$ modification over a length scale on the order of δ, and second, the shape of the bubble far from the wall shows an $O(\delta)$ modification.

We also developed a theory for the streaming flow in such a domain, which accommodates the appropriate boundary conditions at both the bubble and the wall. The flow in the bulk is independent of the value of δ to leading order, and is a function only of the shape of the bubble oscillations. It must be noted however, that the exponent of the dominant radial decay in the far-field is independent of the shape of oscillation of the bubble. While the theory qualitatively agrees with experimental observations for purely radial oscillations of the bubble surface, it only weakly captures the effect of surface mode oscillations on the streaming.

A possible cause for the anomaly between the theory and experiment is that the jump in the radial velocity between the wall and the bubble surface is not properly handled by the eigenfunction expansion employed. We have also neglected the effect of the finite boundary layer thickness on the mean flow in the bulk, as stated earlier. If parallels are to be drawn with the classical case of the oscillating cylinder, the leading order solution might be expected to diverge from the exact solution as δ increases from zero [8]. A third challenge is that one can only speculate on the boundary conditions at the bubble surface. While the kinematic condition is trivial, the stress-free condition is much harder to verify and may, in general, be modified by the presence of surfactants or impurities at the interface.

CHAPTER 3

DYNAMICS OF OSCILLATION

3.1 Introduction

In the preceding chapter we discussed the family of allowable oscillations of a cylindrical bubble pinned to a solid surface, the family of allowed oscillatory flows, and the resulting family of streaming flows. In this chapter, we explore a mechanism of exciting such an oscillation using an oscillatory far field pressure, and attempt to describe the shape of the bubble oscillations as a function of the driving frequency. In a classical paper, Plesset [18] explores a non-linear mechanism of coupling between radial oscillation and a surface perturbations for a spherical bubble in free space, which produces a plethora of interesting non-linear behaviour [19]. In the linear limit, however, each surface mode behaves as a linear oscillator, but is decoupled from volume oscillations of the bubble. In principle, one may couple the individual surface modes by imposing a pinning condition, as has been done for a pinned spherical bubble [17, 20, 21]. However, to properly deal with contact line dynamics, one must treat carefully the viscous region near the wall. Here we present a mechanism for linear coupling between oscillation modes that is contingent only on the geometry of the bubble at rest. Through the analysis, we consider only the the region of the domain outside of the wall boundary layer, and therefore do not impose a condition on the contact line, as has been elaborated on in Subsection 2.5.2.

3.2 Problem definition

Since it is often desirable in experiment to optimize the geometry of the setup depending on the exact application, we consider here a geometry that

is a generalization of the one described in Chapter 2. Consider a cylindrical bubble of infinite axial extent, with a radius a. The surface of the bubble is in contact with two rigid no-slip plane surfaces, which when extended, intersect at an axis O that is offset from the axis of the bubble C by a distance ξa. The quantity ξ is defined positive if O is farther away from the the the wall than C. One may define a polar coordinate system whose axis coincides with the axis of intersection of the walls, and define the angular coordinate θ such that one of the surfaces is described by $\theta = 0$ and the other by $\theta = 2\beta$. We assume that the volume of the side channel below the line joining the two corners, enclosed between the walls, is given as $V_d = 1/2\pi a^2\alpha$, and will refer to it as the "dead volume", α being a geometrically determined constant. The exterior of the bubble contains a fluid of constant density ρ and dynamic viscosity μ, and the gas inside the bubble is assumed to have negligible density and viscosity in comparison with the external fluid.

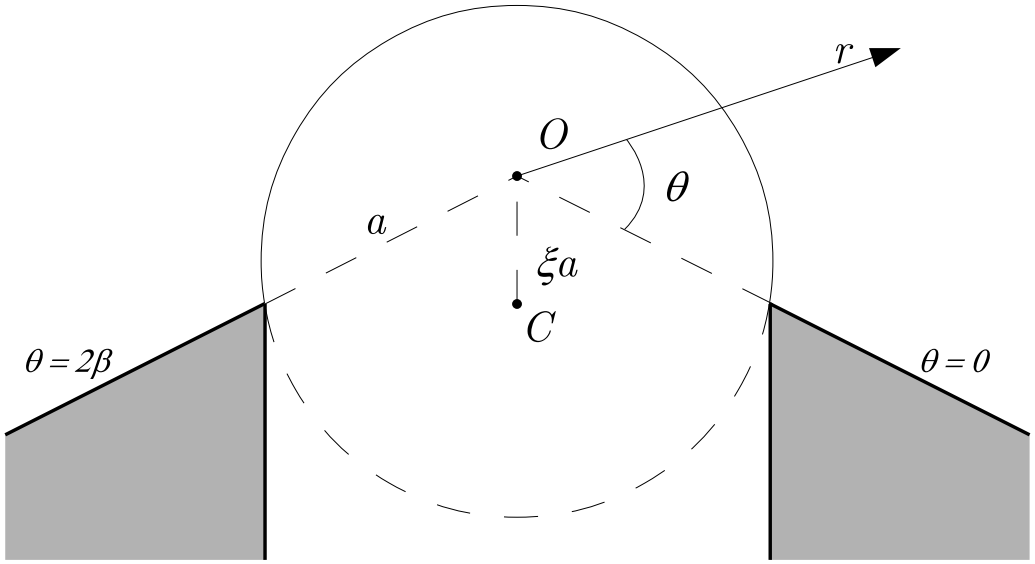

Figure 3.1: Definition of Coordinates for an Oscillating Pinned Bubble

In the linear limit, one may assume that the surface of the bubble undergoes small amplitude oscillations of a single temporal angular frequency ω about its rest position and has the form

$$R(\theta) = a(f(\theta) - iz(\theta)e^{i\omega t}), \tag{3.1}$$

where $f(\theta)$ is the distance of the rest bubble surface from the origin, and $z(\theta)$ here is small in comparison with unity. If the mean rest shape of the

bubble is symmetric with respect to $\theta = \beta$, we have

$$f(\theta) = \sqrt{1 - \xi^2 \sin^2(\theta - \beta)} - \xi \cos(\theta - \beta). \tag{3.2}$$

3.3 External flow field

If the Reynolds number associated with the oscillatory flow is large, viscous effects are confined to a thin oscillatory boundary layer of characteristic thickness δ near the boundaries. The external flow field is then irrotational and may be described by a potential, as we have discussed in Chapter 2. We define a velocity potential $\varphi(r, \theta)$ such that

$$\mathbf{u} = \nabla\varphi.$$

The velocity potential is a harmonic function for incompressible flow and satisfies

$$\nabla^2\varphi = 0. \tag{3.3}$$

We require that the velocity field produced by φ remain bounded at infinity, and that it does not penetrate the walls, which provides the boundary conditions

$$\frac{\partial\varphi}{\partial\theta}(r, \theta = 0) = \frac{\partial\varphi}{\partial\theta}(r, \theta = 2\beta) = 0. \tag{3.4}$$

The general solution to the Eq.(3.3) with the boundary conditions Eq.(3.4) is

$$\varphi(r, \theta) = a^2\omega \left(A_0 \log\left(\frac{a}{r}\right) + \sum_{n=1}^{\infty} \frac{A_n}{m} \frac{a^m}{r^m} \cos(m\theta) \right) e^{i\omega t}, \tag{3.5}$$

where $m = n\pi/(2\beta)$, the coefficients A_n are in general, complex and $|A_n| \ll 1$.

If the time dependent surface of the bubble is described by $\mathcal{F} = r - R(\theta, t) = 0$, the continuity of normal velocity at the bubble surface gives

$$\frac{D\mathcal{F}}{Dt} = 0,$$

which reduces to a kinematic condition at the surface of the bubble

$$\frac{\partial R}{\partial t} = \frac{\partial\phi}{\partial r} - \frac{1}{a}\frac{f'}{f^2}\frac{\partial\phi}{\partial\theta}, \quad r = R \tag{3.6}$$

To leading order in the oscillation amplitudes, the kinematic boundary condition in (3.6) may be applied at the mean bubble surface $r = af(\theta)$ which gives a general expression for the shape of the bubble surface oscillation

$$z(\theta) = -\frac{1}{f}\sum_{n=0}^{\infty}\frac{A_n}{f^m}\left\{\cos m\theta - \frac{f'}{f}\sin m\theta\right\} \tag{3.7}$$

3.4 Dynamic pressure balance across the interface

The interface is in dynamic equilibrium due a balance of pressure, and normal stresses due to viscosity and surface tension. The external pressure is entirely a consequence of the flow field and the imposed pressure at infinity, while the internal pressure is primarily due to the volume oscillations of the bubble.

$$p^i = p^e - \tau + \sigma\kappa, \tag{3.8}$$

where p is the pressure, τ is the viscous stress normal to the interface, σ is the surface tension and κ is the mean surface curvature.

3.4.1 Surface Tension

For a curve $R(\theta)$ in polar coordinates, the curvature is given by

$$\kappa = \frac{R^2 + 2R'^2 - RR''}{(R^2 + R'^2)^{3/2}},$$

which may be linearized for $z(\theta) \ll 1$ to yield

$$\begin{aligned}\kappa \sim \frac{1}{aF_1^{3/2}}\Bigg[&F_2 + i\left\{\left(3\frac{F_2}{F_1} - 2\right)f + f''\right\}ze^{i\omega t} \\ &+ i\left\{3\frac{F_2}{F_1} - 4\right\}f'z'e^{i\omega t} + ifz''e^{i\omega t}\Bigg],\end{aligned} \tag{3.9}$$

where the functions F_1 and F_2 are defined as

$$\begin{aligned}F_1(\theta) =& f^2 + f'^2, \text{ and} \\ F_2(\theta) =& f^2 + 2f'^2 - ff''\end{aligned}$$

Using the rest bubble shape $f(\theta)$ in (3.2) and the general form of the shape oscillation $z(\theta)$ in Eq.(3.7), we have, to $O(\xi)$,

$$a\,\kappa(\theta) \sim 1 + ie^{i\omega t}\sum_{n=0}^{\infty} A_n \Bigg[\kappa_1(m)\cos m\theta \\ - \xi\Big\{\kappa_2(m)\cos\left((m-1)\theta+\beta\right) - \kappa_3(m)\cos\left((m+1)\theta-\beta\right)\Big\}\Bigg], \tag{3.10}$$

where

$$\begin{aligned}
\kappa_1(m) &= (m+1)(m-1) + \frac{\xi^2}{4}m(m+1)(m^2+7m+4),\\
\kappa_2(m) &= -\frac{1}{2}m(m+1)(m-1),\\
\kappa_3(m) &= \frac{1}{2}m(m+1)(m+5)
\end{aligned} \tag{3.11}$$

In the interest of projecting the normal stress due to surface tension onto an orthogonal basis, Eq.(3.10) for the curvature may be written as

$$\kappa(\theta) = \frac{1}{a} + \frac{1}{a}ie^{i\omega t}\sum_{n=0}^{\infty}\mathbb{K}_n\cos(m\theta), \tag{3.12}$$

where

$$\mathbb{K}_n = \frac{\langle\kappa(\theta),\cos(m\theta)\rangle}{\langle\cos(m\theta),\cos(m\theta)\rangle}$$

The inner product used here is similar to the one defined in Chapter 2 except that the limits of integration range from $\theta = 0$ to $\theta = 2\beta$.

3.4.2 Pressure

The pressure anywhere in the domain is given to leading order in $z(\theta)$ by the linearized Bernoulli equation

$$p(\boldsymbol{x},t) = P_0 + p_0(t) - \rho\frac{\partial\varphi}{\partial t}(\boldsymbol{x},t),$$

where P_0 is the steady ambient pressure and p_0 is an oscillatory uniform pressure. Note that the pressure associated with the flow field, given by

$$\begin{aligned} p_f(r,\theta) =& -\rho\frac{\partial\phi}{\partial t} \\ =& -i\rho a^2\omega^2\left(A_0\log\left(\frac{a}{r}\right)+\sum_{n=1}^{\infty}\frac{A_n}{m}\frac{a^m}{r^m}\cos m\theta\right)e^{i\omega t} \end{aligned} \tag{3.13}$$

diverges logarithmically as $r\to\infty$, and is a consequence of having a two dimensional monopole. This problem does not arise for an oscillating bubble with a finite axial dimension. We resolve the issue by assuming that the pressure associated with the oscillatory monopole at infinity may be effectively evaluated at a radius $r = aR_\infty$. We assume that R_∞ is sufficiently large, so that the contributions of the surface modes to the pressure is negligible at this distance from the bubble. The total pressure at infinity is then given by

$$p(r\to\infty,\theta)\sim P_0+p_0(t)+i\rho a^2\omega^2 e^{i\omega t}A_0\log\left(\frac{1}{R_\infty}\right).$$

The pressure at the moving interface may be evaluated, to leading order in the oscillation amplitude at the mean bubble surface, $r = af(\theta)$. We then have

$$\begin{aligned} p_e(\theta) \sim& P_0+p_0(t)+i\rho a^2\omega^2 e^{i\omega t}A_0\log\left(\frac{1}{R_\infty}\right)-\rho\frac{\partial\phi}{\partial t}\bigg|_{r=af(\theta)} \\ =& P_0+p_0(t) \\ & -i\rho a^2\omega^2 e^{i\omega t}\left(A_0\log\left(\frac{R_\infty}{f}\right)+\sum_{n=1}^{\infty}\frac{A_n}{m}\frac{1}{f^m}\cos m\theta\right) \end{aligned} \tag{3.14}$$

which may be expanded as

$$\begin{aligned} p_e(\theta) \sim& P_0+p_0(t)+i\rho a^2\omega^2 e^{i\omega t}A_0\log\left(\frac{1}{R_\infty}\right) \\ & -i\rho a^2\omega^2 e^{i\omega t}\sum_{n=0}^{\infty}A_n\Big[p_1(m)\cos m\theta \\ & -\xi\Big\{p_2(m)\cos\left((m-1)\theta+\beta\right)-p_3(m)\cos\left((m+1)\theta-\beta\right)\Big\}\Big]. \end{aligned} \tag{3.15}$$

where

$$p_1(m) = \begin{cases} 0 & , m = 0 \\ \dfrac{1}{m} & , m > 0 \end{cases}$$
$$p_2(m) = -p_3(m) = -\frac{1}{2}. \tag{3.16}$$

The equation (3.14) for the pressure is projected on the orthogonal basis of cosines

$$p_e(\theta) = P_0 + p_0(t) - i\rho a^2 \omega^2 e^{i\omega t} \sum_{n=0}^{\infty} \mathbb{P}_n \cos(m\theta), \tag{3.17}$$

where

$$\mathbb{P}_n = \frac{\langle p_e - P_0 - p_0, \cos(m\theta) \rangle}{\langle \cos(m\theta), \cos(m\theta) \rangle}.$$

The pressure on the bubble surface exerted by the gas in its interior consists of a contribution from its volume change and one due to the internal flow field. However, if the density of the gas inside the bubble is much smaller than that of the density of the liquid outside of it, the pressure associated with the internal flow is negligible compared to that produced by the external flow and as a consequence the internal bubble pressure is uniform for all practical purposes. Assuming an ideal gas at a constant temperature, we have that the change in internal bubble pressure p_i is related to the change in the volume of the gas v_i as

$$p_i = -v_i \frac{P_i}{V_i},$$

where P_i and V_i are the internal pressure and the volume of the bubble at rest. The internal rest volume is easily evaluated from geometry. The change in volume is given, to leading order, by

$$v_i = \int_0^{2\beta} -iz(\theta) e^{i\omega t} f(\theta)\, d\theta.$$

If the pressure jump between the external and the internal ambient pressures due to surface tension is small, we find that the oscillatory pressure of the

gas in the bubble is given by

$$\begin{aligned} p_i \sim & -2i\beta P_0 A_0 e^{i\omega t}\left[\frac{1}{\alpha+\beta}+\frac{2\xi\sin\beta}{(\alpha+\beta)^2}\right] \\ = & -i\frac{\sigma}{a}e^{i\omega t}\Pi. \end{aligned} \tag{3.18}$$

3.4.3 Viscous stress

In a potential flow, viscous stresses vanish everywhere except at discontinuity surfaces [22]. For a general flow field, the viscous stress τ normal to a surface ∂S with unit normal $\boldsymbol{n}$ are given by

$$\tau = \boldsymbol{n}.\boldsymbol{\Sigma}.\boldsymbol{n},$$

where $\boldsymbol{\Sigma}$ is the viscous stress tensor, given by

$$\boldsymbol{\Sigma} = \mu\left(\nabla\boldsymbol{u}+\nabla\boldsymbol{u}^T\right)\Big|_{\partial S}. \tag{3.19}$$

For a surface described by $\mathcal{F}=0$, we have

$$\boldsymbol{n} = \frac{\nabla\mathcal{F}}{|\nabla\mathcal{F}|}. \tag{3.20}$$

To leading order in the oscillation amplitude, the unit normal and the viscous stress tensor may be evaluated at the rest bubble surface, to give, for the viscous normal stresses,

$$\begin{aligned} \tau(\theta) \sim \mu\omega e^{i\omega t}\sum_{n=0}^{\infty} A_n\Big[&\tau_1(m)\cos m\theta \\ &-\xi\Big\{\tau_2(m)\cos\left((m-1)\theta+\beta\right)-\tau_3(m)\cos\left((m+1)\theta-\beta\right)\Big\}\Big], \end{aligned} \tag{3.21}$$

where

$$\begin{aligned} \tau_1(m) &= (m+1)\left(2+\frac{1}{2}\xi^2(m^2+6m+4),\right) \\ \tau_2(m) &= -m(m+1), \\ \tau_3(m) &= (m+1)(m+4) \end{aligned} \tag{3.22}$$

The viscous stresses produced by the motion of the gas may be neglected if its dynamic viscosity is much smaller than that of the liquid.

Analogous to the decompositions of the surface tension and the pressure, we may rewrite the expression for the viscous stresses in Eq.(3.21) as

$$\tau(\theta) = \mu\omega e^{i\omega t} \sum_{n=0}^{\infty} \mathbb{T}_n \cos(m\theta), \tag{3.23}$$

where

$$\mathbb{T}_n = \frac{\langle \tau(\theta), \cos(m\theta) \rangle}{\langle \cos(m\theta), \cos(m\theta) \rangle}.$$

The steady component of the dynamic pressure balance in Eq.(3.8) gives the equilibrium pressure jump across the interface $P_i - P_0 = \frac{\sigma}{a}$, and the unsteady component gives

$$p_0(t) + \sum_{n=0}^{\infty} \left\{ -i\rho a^2 \omega^2 \mathbb{P}_n - \mu\omega \mathbb{T}_n + i\frac{\sigma}{a}\mathbb{K}_n \right\} \cos m\theta e^{i\omega t} = -i\frac{\sigma}{a} e^{i\omega t} \Pi.$$

If we assume that the time dependent uniform pressure at infinity has the form $p_0(t) = -i\frac{\sigma}{a}\hat{p}e^{i\omega t}$, we have

$$\Omega^2 \Pi + \sum_{n=0}^{\infty} \left\{ -\omega^2 \mathbb{P}_n + 2i\zeta\Omega\omega\mathbb{T}_n + \Omega^2 \mathbb{K}_n \right\} \cos m\theta = \Omega^2 \hat{p}\,, \tag{3.24}$$

where

$$\begin{aligned} \Omega &= \sqrt{\frac{\sigma}{\rho a^3}}, \text{ and} \\ \zeta &= \frac{\mu}{2\sqrt{\rho a \sigma}}. \end{aligned} \tag{3.25}$$

By the orthogonality of the angular functions in the domain, it follows that Eq.(3.24) may be separated into its native modal dependences. We thus obtain the system of equations

$$-\omega^2 \mathbb{P}_n + 2i\zeta\Omega\omega\mathbb{H}_n + \Omega^2(\mathbb{K}_n + \delta_{0n}\Pi) = \delta_{0n}\Omega^2\hat{p}, \tag{3.26}$$

where n is any non-negative integer and δ_{ij} is the Kronecker delta. It is clear from Eq.(3.26) that the forcing pressure only appears in the equation independent of θ. For $\xi = 0$, the volume mode oscillations are decoupled

from the dynamics of the surface modes, which are therefore not permitted to sustain oscillations in the linear limit. The equation, in this case, describing the dynamics of the surface modes reduces to the result,

$$\left\{-\omega^2 + 4i\zeta\Omega m(m+1)\,\omega + \Omega^2 m(m^2-1)\right\} A_n = 0. \tag{3.27}$$

However, for $\xi \neq 0$, the surface mode dynamics are coupled to the volume oscillation dynamics and are therefore driven by it. It should also be said that by symmetry of the volume oscillations and the assumed symmetry of the rest bubble shape with respect to $\theta = \beta$, bubble shape oscillations of opposite symmetry, denoted by odd values of n, are not coupled to the volume mode and are therefore absent.

It is tempting to decompose the bubble shape in Eq.(3.7) itself into Fourier cosine modes, and so we write

$$z(\theta) = \sum_{n=0}^{\infty} z_n \cos n\theta, \tag{3.28}$$

where

$$z_n = \frac{\langle z(\theta), \cos n\theta \rangle}{\langle \cos n\theta, \cos n\theta \rangle}.$$

Equation (3.24) represents a infinite system of algebraic equations that may be solved for the coefficients A_n as a function of the forcing term $\hat{p}$ and the angular frequency ω, for any given ξ. However, R_∞ may not be determined within the framework of the theory determined here, and therefore a traditional response of the oscillator to a constant forcing is impossible to determine. However, since the system is linear, each of the coefficients A_n is proportional only to the imposed pressure $\hat{p}$ and therefore, one may compute the relative strengths of the coefficients unambiguously, independent of the value of imposed pressure at any given frequency. It follows that the bubble shape $z(\theta)$ given in Eq.(3.7), which is linear in the coefficients A_n, is also subject to a similar normalization. While the absolute amplitudes themselves are determine the overall strength of the streaming flow, the type of steady flow induced depends only on the relative amplitudes of oscillation modes, and therefore a calculation of relative amplitudes and phases is relevant. We define a surface mode amplitude relative to the monopolar amplitude given

by

$$a_n = \frac{|z_n|}{|z_0|}, \tag{3.29}$$

and a relative phase of the surface mode by

$$\phi_n = arg(z_n) - arg(z_0). \tag{3.30}$$

It must be noted that at no point have we imposed that the bubble surface near the wall remain stationary. This is because the potential flow approximation s only valid outside of the bubble boundary layer, and in order to enforce pinning, one must treat the viscous region near the wall. This is consistent with the treatment in Chapter 2, where we have shown that it is possible to have a finite non-zero bubble surface velocity at the edge of the oscillatory wall boundary layer, provided that the wall is everywhere rigid and no-slip.

3.5 Results and comparison with experiment

We apply the analysis in the preceding section to the case of a flat wall, for which $\beta = \pi/2$. Although the governing equations for the mode amplitudes, contained in Eq.(3.26), admit a small degree of simplification for this case, their nature remains unchanged, namely that they represent linear oscillators that are coupled to each other for non-zero values of ξ. We have already commented on the difficulty in determining the absolute amplitudes of oscillation in response to the imposed pressure. This is well, since in experiment, it is difficult to determine the exact pressure delivered to the bubble, which is ultimately dependent on the dynamics of the setup. However, the relative amplitudes, in the linear limit, are independent of the driving pressure and may be determined unambiguously. In order to determine relative amplitudes and phases of surface surface modes, we pick an arbitrary value of A_0 and solve the system of equations represented by Eq.(3.26) for $n \geq 2$. In addition, we assume that a finite number of oscillation modes are present, the highest one corresponding to $n = N$. Consequently, the system of equations in Eq.(3.26) is solved numerically for $2 \leq n \leq N$.

The experimental setup is similar to the one described in Chapter 2, with

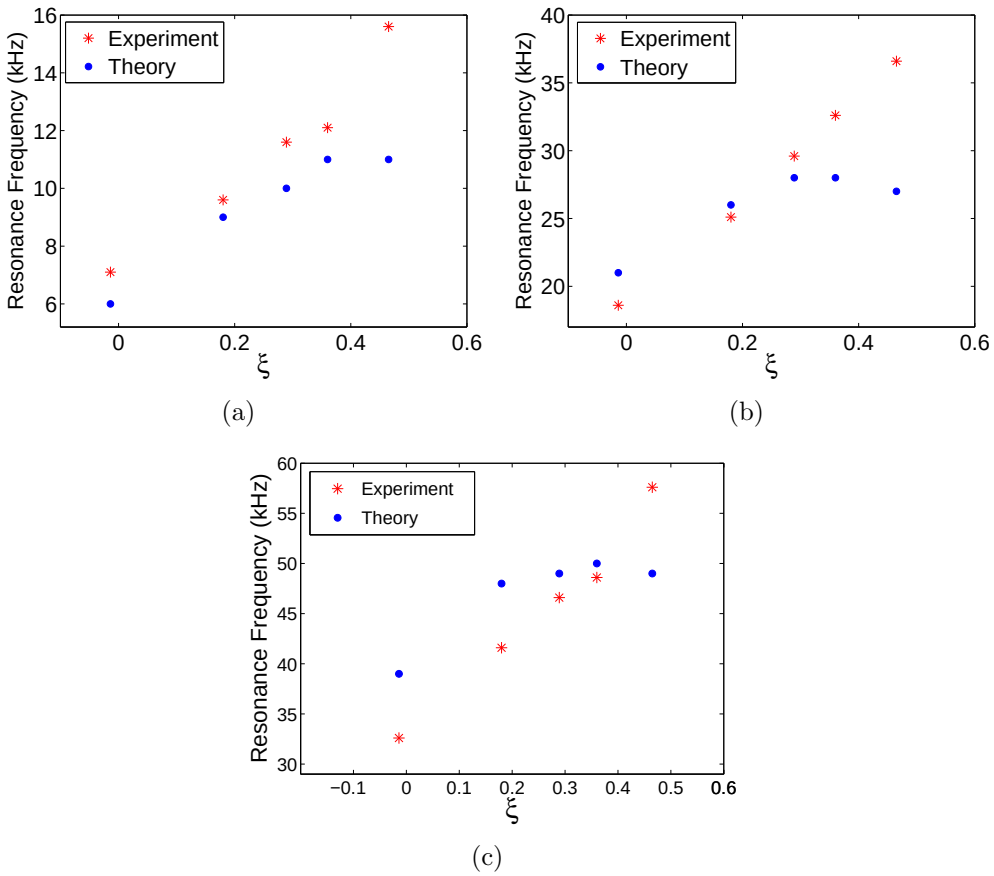

Figure 3.2: Relative amplitude resonance frequencies plotted against ξ for the first three surface modes (a) $n = 2$, (b) $n = 4$, (c) $n = 6$

a bubble enclosing a volume of gas in a side channel of an otherwise fluid-filled main channel. We employ an inverted microscope and a high speed camera for the purposes of visualization and data analysis. Each image of the bubble outline taken by the high speed camera is decomposed into its Fourier components. From a time series of images, the amplitudes and the phases of each Fourier mode of the bubble shape oscillation may be extracted, for any given frequency. We use for our experiment and therefore our calculation, an exterior fluid with dynamic viscosity $\mu = 2 \times 10^{-3} Ns/m^2$ and a density $\rho = 1050 kg/m^3$. The surface tension of the interface is $\sigma = 40 \times 10^{-3} N/m$. The radius of the bubble itself is a function of ξ, but the width of the side channel containing the gas bubble is fixed at 85 microns.

For moderate values of ξ, the resonance frequencies are predicted quite well. The experiments show a clear increase in the peak frequency with ξ,

which the theory captures well, particularly for the lower modes and for lower values of ξ. Since we have used an expansion in ξ accurate to leading order, one expects to encounter some difficulty when ξ is $O(1)$.

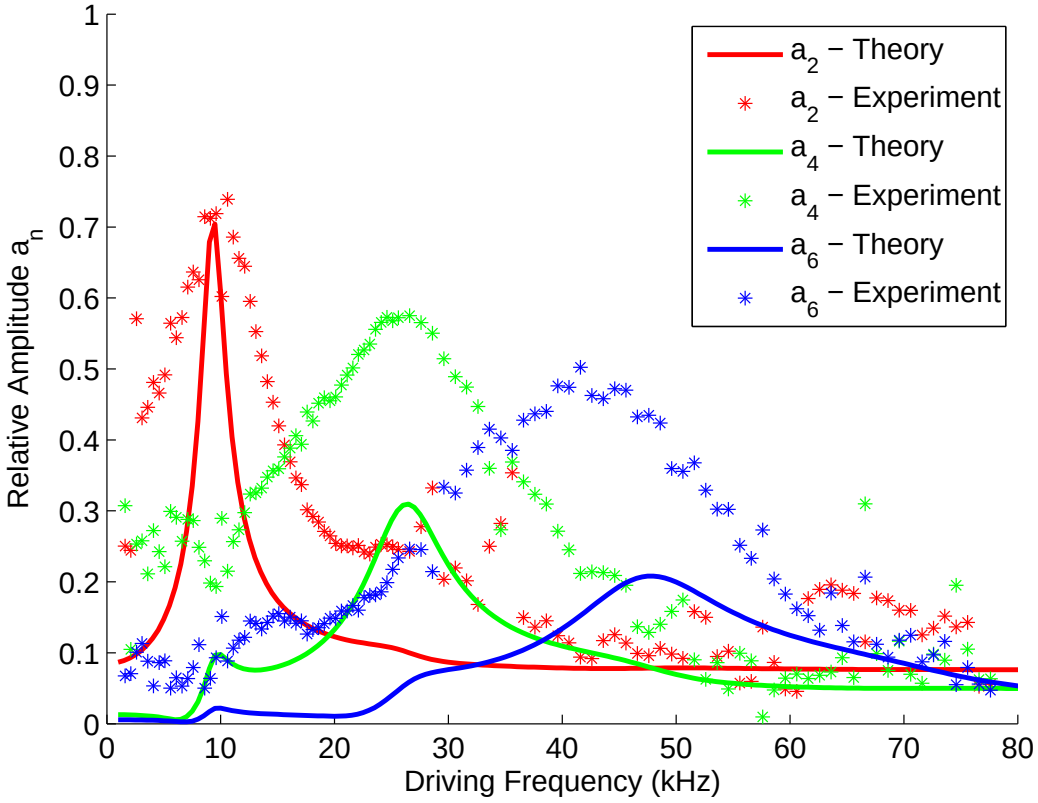

Figure 3.3: Comparison of theoretical predictions and experimental data for the relative amplitudes of the surface modes ϕ_n as a function of the driving frequency for $\xi = 0.18$.

The widths of the relative amplitude curves, however, are underpredicted by the theory by a factor of between 2 and 3. The dependence of the widths of the relative amplitude curves on ξ is much less clear. However, the predictions for relative amplitudes and the widths of the response curves are significantly smaller than the values suggested by the experimental data. In particular, one must note that the relative amplitudes for $\xi = -0.014$ are much smaller than those that are suggested by the experimental data, despite the existence of well defined peaks.

The theoretically predicted relative phase angle is in good agreement with the experimental data up until the resonance frequency, for which the sine of the phase is unity. While the theory predicts a phase response that more

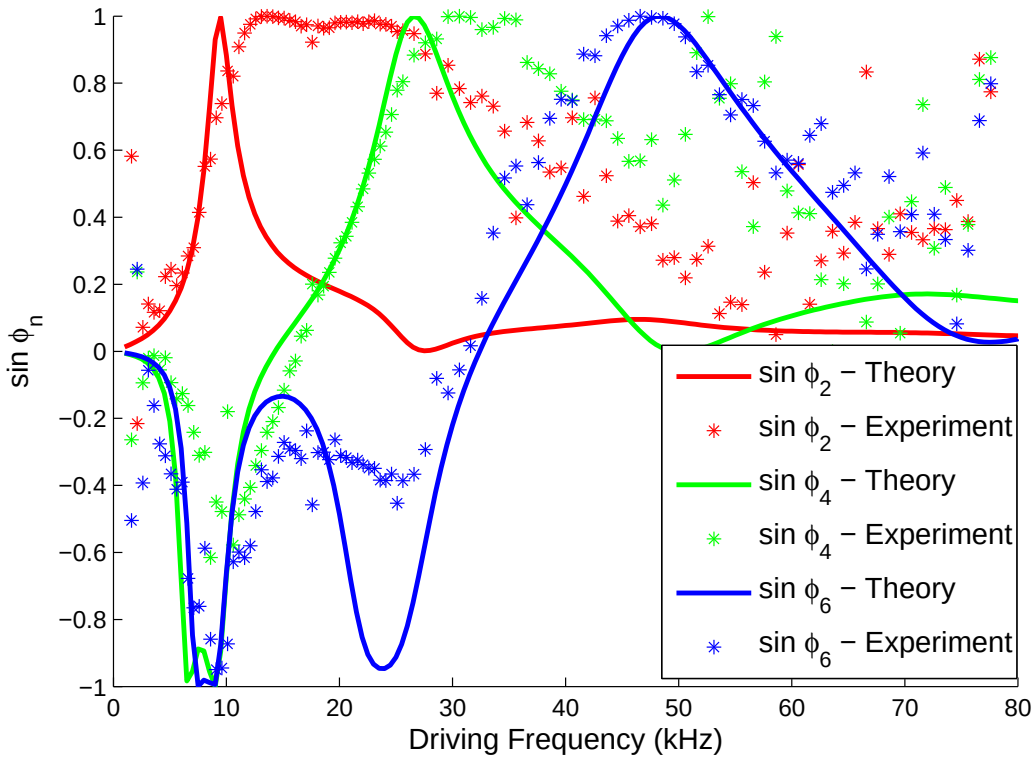

Figure 3.4: Comparison of Theoretical predictions and Experimental data for the sine of the relative phase ϕ_n as a function of the driving frequency for $\xi = 0.18$.

closely resembles that of classical harmonic oscillator, the experimental data shows a marked post-resonance phase plateau. This effect is particularly strong for the first oscillation mode, and diminishes for higher modes.

3.6 Concluding remarks

We have proposed a mechanism for the linear coupling of surface mode oscillations to the volumetric oscillation of the the bubble. The analysis, to some extent predicts resonance frequencies, and captures their dependence on ξ quite well for small values of ξ. However, the overall widening of the response curves, both amplitude and phase is unexplained. It must also be noted that for $\xi = 0$, the theory predicts no sustained surface mode oscillations and the amplitudes. On the contrary, significant surface mode amplitudes may be observed in the experiment even for $\xi \sim -0.014$, for which the theory fails.

It is important to realize here that our negligence of the boundary layer

thickness poses a two-fold problem. First, the modification of the bubble shape effected by the having a finite value of δ, as described in Chapter 2, is discounted. This shape modification would then be capable of driving the oscillator, even for $\xi = 0$. Second, for values of δ that are not negligible in comparison to unity, vortical effects produced by viscosity near the wall may permeate into the bulk of the fluid, and the potential flow approximation may be inadequate. We have also neglected non-linear effects, particularly in the potential from the curvature terms in Subsection 3.4.1, which may modify the frequency response.

CHAPTER 4

CONCLUSIONS

In this work, we have considered two fundamental problems related to oscillation of a cylindrical bubble pinned to a wall. Our main aim was to characterize the response of such a bubble to an applied acoustic field and compute the streaming flow resulting thereof. The theoretical efforts in this work have largely been inspired by the use of acoustically excited microbubbles as efficient manipulators of flow at the micrometer scale.

In the first part of the work, we considered the problem of determining the flow field induced by oscillations of the bubble interface. We were able to produce a very consistent picture of the oscillatory flow field everywhere in the domain, inclusive of the viscous regions over the walls around the bubble and near the contact lines. We then showed that the shape of the bubble must depend on the boundary layer thickness δ, both close to and far away from the rigid wall to which it is pinned. In particular, the shape of the bubble near the wall is corroborated by experimental observations at large driving frequencies.

We proceeded to calculate the leading order streaming flow in the domain, which, to leading order, is dominated by anti-fountain loops arising from having an outward apparent slip velocity near the wall, thereby solving Nyborg's long-standing problem of the steady streaming induced by an oscillating source. The results of the theory agree qualitatively with experimental observations at driving frequencies for which the bubble oscillation is essentially monopolar. In important result here is that the velocity in the bulk of the fluid decays slower than it does along the wall. We find that in experiments, the streaming flow is dominated by fountain loops at frequencies for which surface modes become important. While the theory does predict the emergence of fountain loops, they remain largely confined to a region around the apex of the bubble, and the bulk of the flow is dominated by anti-fountain loops produced as a result of slip along the wall. The inclu-

sion of higher order terms in the boundary layer thickness δ may produce the characteristic flow reversal that we see in experiments, and may be analogous to the case of the oscillating cylinder in bulk fluid [8].

The second part of the work is an attempt at predicting the response of the bubble to a uniform oscillatory pressure at a given temporal frequency. By assuming that the oscillatory flow is irrotational, we have proposed a geometric mechanism by which surface modes may be driven through a linear coupling with volume oscillations of the bubble. While the peak frequencies of the surface modes relative to the volume modes are predicted well, the widths of the response curves are underpredicted by the theory. The theoretical predictions for relative phases are also in good agreement with the experimental data for the higher modes. The experimental data for lower modes, however, show a pronounced post-resonance plateau in the relative phase angle, which is not predicted by the theory. In order to properly span the range of frequencies in which we are interested, it may be necessary to account for vortical effects in the oscillatory flow.

APPENDIX A

A.1 Evaluation of the particular solution to the steady problem

Here we elaborate on the method of evaluating the particular solution to the Eulerian mean flow, by means of an eigenfunction decomposition. We rewrite the governing equation (2.46) for a combination of oscillatory modes m and n.

$$\begin{aligned}\nabla^4 \left\{ {}_m\psi_n^E \right\} &= \frac{2}{\delta^2} \left\langle -\frac{1}{r} \frac{\partial(\psi_0^m, \nabla^2 \psi_0^n)}{\partial(r,\theta)} \right\rangle \\ &= \frac{2}{\delta^2}\, {}_mQ_n \end{aligned} \tag{A.1}$$

where

$$\begin{aligned} {}_mQ_n &= -\left\langle \frac{1}{r} \frac{\partial(\psi_0^m, \nabla^2 \psi_0^n)}{\partial(r,\theta)} \right\rangle \\ &= -\frac{1}{2r} \left[\frac{\partial \psi_0^{*m}}{\partial r} \frac{\partial \nabla^2 \psi_0^n}{\partial \theta} - \frac{\partial \psi_0^{*m}}{\partial \theta} \frac{\partial \nabla^2 \psi_0^n}{\partial r} \right] \end{aligned} \tag{A.2}$$

and the real part is understood everywhere. We recognize that ${}_mQ_n$ decays exponential away from the surface of the bubble over a scale of δ, by virtue of the nature of the oscillatory vorticity that it contains. If we define define a boundary layer coordinate $\eta = (r-1)/\delta$, we may expand the inhomogeneity in powers of δ. Using the form of the oscillatory solution in Eq.(2.44), we find that

$$
\begin{aligned}
{}_mQ_n \sim & -\frac{1}{2}n(n+2)e^{-(1+i)\eta}\sin m\theta\cos n\theta e^{i\phi_{nm}} \\
& + \left[\frac{(1+i)}{2\delta}(2+n)e^{-(1+i)\eta}\right. \\
& \left. - \frac{1}{4}(2+n)\left\{3+(1+i)(2m+3)\eta\right\}\right]\sin n\theta\cos m\theta e^{i\phi_{nm}} \\
= & \, {}_mQ_n^+\sin(m+n)\theta\, e^{i\phi nm} + {}_mQ_n^-\sin(m-n)\theta\, e^{i\phi nm}
\end{aligned}
\tag{A.3}
$$

where $\phi_{nm} = \phi_n - \phi_m$ and

$$
\begin{aligned}
{}_mQ_n^+ &= (n+2)\left[\frac{(1+i)}{4\delta} - \frac{1}{4}n - \frac{1}{8}\left\{3+(1+i)(2m+3)\eta\right\}\right]e^{-(1+i)\eta} \\
{}_mQ_n^- &= (n+2)\left[\frac{(1+i)}{4\delta} + \frac{1}{4}n - \frac{1}{8}\left\{3+(1+i)(2m+3)\eta\right\}\right]e^{-(1+i)\eta}
\end{aligned}
\tag{A.4}
$$

Here, we have expressed the inhomogeneity in a form that is compatible with the exponentially decaying eigenfunctions of the biharmonic operator presented in Eq.(2.48). Our task now is to express ${}_mQ_n$ as a linear combination of eigenfunctions, and doing so, we must choose the correct eigenvalues in order to capture the asymptotic behaviour of the inhomogeneity. The appropriate eigenfunctions are determined from the angular behaviour of the two components of ${}_mQ_n$. It follows then that one may attempt a decomposition of the form

$$
\begin{aligned}
\frac{2}{\delta^2}\,{}_mQ_n^+\sin(m+n)\theta \sim {}_mb_n^+(1+\delta\,{}_m\sigma_n^+)\times & \\
K_{m+n}\left[\left(\frac{(1+i)}{\delta} + {}_m\mu_n^+\right)r\right]\sin(m+n)\theta &
\end{aligned}
\tag{A.5}
$$

where ${}_m\mu_n^+$ is an $O(1)$ quantity. The corresponding eigenvalue ${}_m\lambda_n^+$ and the weight ${}_mp_n^+$ of the eigenfunction in the expansion are

$$
\begin{aligned}
{}_m\lambda_n^+ &= \frac{(1+i)}{\delta} + {}_m\mu_n^+ \\
{}_mp_n^+ &= {}_mb_n^+(1+\delta\,{}_m\sigma_n^+)
\end{aligned}
\tag{A.6}
$$

If we expand the right hand side of Eq.(A.5) for small δ, in the boundary

layer coordinate η near the mean surface of the bubble, we may evaluate ${}_m b_n^+$, ${}_n\sigma_n^+$ and ${}_m\mu_n^+$, by comparing η dependences at each order of δ.

$$
\begin{aligned}
{}_m b_n^+ =& \frac{\sqrt{\delta}\,(1+i)^{3/2}(n+2)}{\delta^4\sqrt{2\pi}} \exp\left\{\frac{(1+i)}{\delta} + {}_m\mu_n^+\right\} \\
{}_m\mu_n^+ =& 1+m \\
{}_m\sigma_n^+ =& -\frac{(1-i)}{16}(7-4m+4m^2+8n+8mn+4n^2)
\end{aligned}
\tag{A.7}
$$

It follows that the particular solution to the equation

$$
\nabla^4\left\{{}_m\psi_n^+\right\} = \frac{2}{\delta^2}\,{}_m Q_n^+ \sin(m+n)\theta
$$

is then given by

$$
{}_m\psi_n^+ = {}_m p_n^+\,({}_m\lambda_n^+)^{-4} K_{m+n}[{}_m\lambda_n^+ r] \tag{A.8}
$$

The term ${}_m Q_n^-$ may be treated in a similar manner, and consequently, the particular solution to Eq.(A.1) is given by

$$
\psi_{m,n} = {}_m\psi_n^+ + {}_n\,\psi_m^-
$$

The solution we have obtained reflects the accuracy of the eigenfunction expansion used. We therefore rewrite the solution in terms of η, accurate to the consistent order in δ, to obtain after simplification,

$$
\begin{aligned}
{}_m\psi_n^E =& A_m A_n \left[-\frac{\delta}{4}(1+i)(2+n)e^{-(1+i)\eta}\right. \\
&\left. + \frac{\delta^2}{8}(2+n)\left\{11+8m+(1+i)(3+2m)\eta\right\}e^{-(1+i)\eta}\right] \\
&\qquad e^{i\phi_{nm}}\sin n\theta\cos n\theta \\
&+ A_m A_n \frac{\delta^2}{4} n(2+n)e^{-(1+i)\eta}e^{i\phi_{nm}}\sin m\theta\,\cos n\theta
\end{aligned}
\tag{A.9}
$$

Despite the fact that the eigenfunction expansion employed is not unique, the solution obtained is, as it should be. The method is easily extended to higher order accuracy in δ, for which ${}_m Q_n^+$ and ${}_m Q_n^-$ must each be decomposed into a number of modified Bessel functions, rather than just one.

A.2 Boundary conditions at the bubble interface

Here we derive the boundary conditions that must be satisfied by the steady flow at the bubble surface. We assume that the bubble surface executes time periodic motion of the form

$$R(\theta, t) = 1 - i\epsilon z(\theta) e^{it} \tag{A.10}$$

where $z(\theta)$ is an arbitrary complex valued functions. We assume the bubble surface is everywhere free of tangential stress. We rewrite the boundary conditions at the bubble surface presented in Eq.(2.23)

$$\left.\begin{aligned} &\frac{1}{r}\frac{\partial \psi}{\partial \theta} = z(\theta) e^{it} \\ &\frac{\partial^2 \psi}{\partial r^2} - \frac{1}{r}\frac{\partial \psi}{\partial r} = 0 \end{aligned}\right\} r = R = 1 - i\epsilon z(\theta) e^{it} \tag{A.11}$$

We express the stream function ψ in an asymptotic series

$$\psi = \psi_0 + \epsilon \psi_1 + O(\epsilon^2)$$

To evaluate the boundary conditions at the moving interface, we first expand the stream function in a Taylor series about $r = 1$. We have, to $O(\epsilon)$,

$$\psi(R, \theta) \sim \psi(1, \theta) - i\epsilon z(\theta) e^{it} \frac{\partial \psi}{\partial r}(1, \theta) \tag{A.12}$$

We first evaluate the kinematic boundary condition.

$$\begin{aligned} \left.\frac{1}{r}\frac{\partial \psi}{\partial \theta}\right|_{r=R} &\sim \left(1 + i\epsilon z e^{it}\right) \frac{\partial}{\partial \theta}\left(\psi - i\epsilon z e^{it}\frac{\partial \psi}{\partial r}\right)_{r=1} \\ &\sim \left(\frac{\partial \psi}{\partial \theta} + i\epsilon z e^{it}\frac{\partial \psi}{\partial \theta} - i\epsilon z e^{it}\frac{\partial^2 \psi}{\partial \theta \partial r} - i\epsilon z' e^{it}\frac{\partial \psi}{\partial r}\right)_{r=1} \\ &= z e^{it} \end{aligned} \tag{A.13}$$

Similarly, for the no-stress boundary condition, we obtain

$$\begin{aligned}\left.\frac{\partial^2\psi}{\partial r^2}-\frac{1}{r}\frac{\partial\psi}{\partial r}\right|_{r=R} &\sim \left.\frac{\partial^2\psi}{\partial r^2}-(1+i\epsilon z e^{it})\frac{\partial\psi}{\partial r}-i\epsilon z e^{it}\left(\frac{\partial^3\psi}{\partial r^3}-\frac{\partial^2\psi}{\partial r^2}\right)\right|_{r=1}\\ &\sim \left.\frac{\partial^2\psi}{\partial r^2}-\frac{\partial\psi}{\partial r}-i\epsilon z e^{it}\left(\frac{\partial^3\psi}{\partial r^3}-\frac{\partial^2\psi}{\partial r^2}+\frac{\partial\psi}{\partial r}\right)\right|_{r=1}\\ &= 0 \end{aligned} \tag{A.14}$$

To leading order, we have boundary conditions for the leading order stream function

$$\left.\begin{aligned}\frac{1}{r}\frac{\partial\psi_0}{\partial\theta} &= z(\theta)e^{it}\\ \frac{\partial^2\psi_0}{\partial r^2}-\frac{1}{r}\frac{\partial\psi_0}{\partial r} &= 0\end{aligned}\right\} r=1 \tag{A.15}$$

To obtain boundary conditions for the steady streaming, we time average the boundary conditions is equations (A.13) and (A.14) to obtain

$$\left.\begin{aligned}\frac{\partial\psi^E}{\partial\theta} &= \left\langle i\epsilon z e^{it}\frac{\partial^2\psi_0}{\partial r\partial\theta}\right\rangle+\left\langle i\epsilon z' e^{it}\frac{\partial\psi_0}{\partial r}\right\rangle\\ \frac{\partial^2\psi^E}{\partial r^2}-\frac{\partial\psi^E}{\partial r} &= \left\langle i\epsilon z e^{it}\frac{\partial^3\psi_0}{\partial r^3}\right\rangle\end{aligned}\right\} r=1 \tag{A.16}$$

where we have also used simplifications from Eq.(A.15). Note that the steady component of the secondary stream function ψ^E represents the Eulerian streaming. We may go a step further and obtain boundary conditions on the Lagrangian mean streaming ψ^L by and addition of a Stokes drift ψ^d to the Eulerian streaming ψ^E.

The steady component of the Stokes drift is given, to $O(\epsilon)$ by

$$\psi^d = \frac{1}{r}\left\langle -i\frac{\partial\psi_0}{\partial\theta}\frac{\partial\psi_0}{\partial r}\right\rangle \tag{A.17}$$

Using Eq.(A.15), we find for the tangential derivative of the Stokes drift,

$$\left.\frac{\partial \psi^d}{\partial \theta}\right|_{r=1} = \frac{1}{r}\left\langle -i\frac{\partial^2 \psi_0}{\partial \theta^2}\frac{\partial \psi_0}{\partial r}\right\rangle_{r=1} + \frac{1}{r}\left\langle -i\frac{\partial \psi_0}{\partial \theta}\frac{\partial^2 \psi_0}{\partial r \partial \theta}\right\rangle_{r=1}$$

$$= -\left\langle i\epsilon z e^{it}\frac{\partial^2 \psi_0}{\partial r \partial \theta}\right\rangle_{r=1} - \left\langle i\epsilon z' e^{it}\frac{\partial \psi_0}{\partial r}\right\rangle_{r=1} \tag{A.18}$$

Similarly, using only the no-stress boundary condition satisfied by the oscillatory flow at the bubble surface, one can show, after some algebra, that

$$\left.\frac{\partial^2 \psi^d}{\partial r^2} - \frac{\partial \psi^d}{\partial r}\right|_{r=1} = \left(\frac{\partial^2}{\partial r^2} - \frac{\partial}{\partial r}\right)\left(\frac{1}{r}\left\langle -i\frac{\partial \psi_0}{\partial \theta}\frac{\partial \psi_0}{\partial r}\right\rangle\right)_{r=1}$$

$$= -\left\langle i\epsilon z e^{it}\frac{\partial^3 \psi_0}{\partial r^3}\right\rangle_{r=1} \tag{A.19}$$

It follows from equations (A.16) (A.18) and (A.19) that the Lagrangian mean flow is no-penetration and no-stress at the mean surface of the bubble.

$$\left.\begin{aligned} &\frac{1}{r}\frac{\partial \psi^L}{\partial \theta} = 0 \\ &\frac{\partial^2 \psi^L}{\partial r^2} - \frac{1}{r}\frac{\partial \psi^L}{\partial r} = 0 \end{aligned}\right\} r = 1 \tag{A.20}$$

REFERENCES

[1] D. Ahmed, X. Mao, J. Shi, B. Juluri, and T. Huang, "A millisecond micromixer via single-bubble-based acoustic streaming," *Lab on a Chip*, vol. 9, no. 18, pp. 2738–2741, 2009.

[2] P. Marmottant and S. Hilgenfeldt, "Controlled vesicle deformation and lysis by single oscillating bubbles," *Nature*, vol. 423, no. 6936, pp. 153–156, 2003.

[3] C. Wang, S. Jalikop, and S. Hilgenfeldt, "Size-sensitive sorting of microparticles through control of flow geometry," *Applied Physics Letters*, vol. 99, p. 034101, 2011.

[4] J. Holtsmark, I. Johnsen, T. Sikkeland, and S. Skavlem, "Boundary layer flow near a cylindrical obstacle in an oscillating, incompressible fluid," *The Journal of the Acoustical Society of America*, vol. 26, p. 26, 1954.

[5] S. Skavlem and S. Tjötta, "Steady rotational flow of an incompressible, viscous fluid enclosed between two coaxial cylinders," *The Journal of the Acoustical Society of America*, vol. 27, p. 26, 1955.

[6] A. Bertelsen, A. Svardal, and S. Tjøtta, "Nonlinear streaming effects associated with oscillating cylinders," *Journal of Fluid Mechanics*, vol. 59, no. 03, pp. 493–511, 1973.

[7] C. Wang, "On high-frequency oscillatory viscous flows," *Journal of Fluid Mechanics*, vol. 32, no. Part 1, pp. 55–68, 1968.

[8] B. Lutz, J. Chen, and D. Schwartz, "Hydrodynamic tweezers: 1. noncontact trapping of single cells using steady streaming microeddies," *Analytical Chemistry*, vol. 78, no. 15, pp. 5429–5435, 2006.

[9] M. Longuet-Higgins, "Viscous streaming from an oscillating spherical bubble," *Proceedings of the Royal Society of London. Series A: Mathematical, Physical and Engineering Sciences*, vol. 454, no. 1970, pp. 725–742, 1998.

[10] W. Nyborg, "Acoustic streaming near a boundary," *The Journal of the Acoustical Society of America*, vol. 30, no. 4, pp. 329–339, 1958.

[11] C. Wang, S. V. Jalikop, and S. Hilgenfeldt, "Flow patterns of microbubble streaming in microfluidic settings," *Bulletin of the American Physical Society*, vol. 56, no. 18, G18.00004, 2011.

[12] N. Riley, "Oscillatory viscous flows. review and extension," *IMA Journal of Applied Mathematics*, vol. 3, no. 4, pp. 419–434, 1967.

[13] N. Riley, "Steady streaming," *Annual Review of Fluid Mechanics*, vol. 33, no. 1, pp. 43–65, 2001.

[14] N. Riley, "The steady streaming induced by a vibrating cylinder," *Journal of Fluid Mechanics*, vol. 68, no. 04, pp. 801–812, 1975.

[15] J. Stuart, "Double boundary layers in oscillatory viscous flow," *Journal of Fluid Mechanics*, vol. 24, no. 4, pp. 673–687, 1966.

[16] W. Raney, J. Corelli, and P. Westervelt, "Acoustical streaming in the vicinity of a cylinder," *The Journal Of The Acoustical Society of America*, vol. 26, p. 1006, 1954.

[17] M. Strani and F. Sabetta, "Free vibrations of a drop in partial contact with a solid support," *Journal of Fluid Mechanics*, vol. 141, pp. 233–247, 1984.

[18] M. Plesset, "On the stability of fluid flows with spherical symmetry," *Journal of Applied Physics*, vol. 25, no. 1, pp. 96–98, 1954.

[19] M. Plesset and A. Prosperetti, "Bubble dynamics and cavitation," *Annual Review of Fluid Mechanics*, vol. 9, no. 1, pp. 145–185, 1977.

[20] I. Fayzrakhmanova and A. Straube, "Stick-slip dynamics of an oscillated sessile drop," *Physics of Fluids*, vol. 21, p. 072104, 2009.

[21] I. Fayzrakhmanova, A. Straube, and S. Shklyaev, "Bubble dynamics atop an oscillating substrate: Interplay of compressibility and contact angle hysteresis," *Physics of Fluids*, vol. 23, p. 102105, 2011.

[22] D. Joseph, "Potential flow of viscous fluids: Historical notes," *International Journal of Multiphase Flow*, vol. 32, no. 3, pp. 285–310, 2006.